Canadian Science Publishing | Canadian Journal of Forest Research

Spruce budworm defoliation patterns during outbreak rise are influenced by tree species, insecticide spraying, and spatial autocorrelation

Journal:	*Canadian Journal of Forest Research*
Manuscript ID	cjfr-2024-0269.R2
Manuscript Type:	Research Article
Date Submitted by the Author:	15-Jan-2025
Complete List of Authors:	Donovan, Shawn David; University of New Brunswick, Faculty of Forestry and Environmental Mgmt MacLean, David; University of New Brunswick, Faculty of Forestry and Environmental Mgmt Hennigar, Chris; University of New Brunswick, Faculty of Forestry and Environmental Mgmt Johns, Rob; Natural Resources Canada, Canadian Forest Service, Atlantic Forestry Centre Zhang, Yun; University of New Brunswick, Faculty of Geodesy and Geomatics Engineering
Is the manuscript for consideration in a Special Issue or Collection?:	Not applicable (regular submission)
Keyword:	current and cumulative defoliation, mixed-effects modelling, cluster analysis, Abies balsamea, Picea glauca

Spruce budworm defoliation patterns during outbreak rise are influenced by tree species, insecticide spraying, and spatial autocorrelation

Shawn D. Donovan[a*], David A. MacLean[a], Chris Hennigar[a], Rob C. Johns[b], Yun Zhang[c]

[a] Faculty of Forestry and Environmental Management, University of New Brunswick, P.O. Box 4400, Fredericton, NB E3B 5A3, Canada

[b] Natural Resources Canada, Canadian Forest Service - Atlantic Forestry Centre, P.O. Box 4000, Fredericton, NB E3B 5P7, Canada

[c] Department of Geodesy and Geomatics Engineering, University of New Brunswick, P.O. Box 4400, Fredericton, NB E3B 5A3, Canada

[*]Corresponding author: Shawn D. Donovan (email: shawn.donovan@unb.ca)

Abstract

Spruce budworm (SBW; *Choristoneura fumiferana* Clem.) outbreaks are an important natural disturbance in North America, killing trees over millions of hectares. We related 11 years of SBW defoliation in 87 plots in Gaspé Peninsula, Québec, to 23 stand, site, and climate variables. Defoliation was consistently ordered among host species: balsam fir > white spruce > black spruce. Within the relatively small 200 km^2 study area, cluster analyses resulted in four and 10 clusters for balsam fir cumulative and current defoliation, respectively; variation in cumulative defoliation converged over 11 years. Current defoliation was significantly spatially autocorrelated among plots within stands, but autocorrelation weakened at distances >2500m. Cumulative defoliation was significantly related to insecticide spraying, minimum and maximum summer temperature, and interactions between SBW larvae per branch versus hardwood and white spruce basal area. Tree species, insecticide spraying, and number of defoliating SBW larvae were the main determinants of defoliation. Results showed much higher local spatial variability in current defoliation patterns than previous studies, but over the course of an outbreak, cumulative defoliation patterns converged. Cumulative defoliation patterns similar to these, assigned based on local defoliation severity, can be input into defoliation-based growth models to predict impacts on growth and survival.

Keywords: current and cumulative defoliation, mixed-effects modelling, cluster analysis, *Abies balsamea*, *Picea glauca*

Introduction

Large-scale insect outbreaks are a major disturbance that impacts forests, reducing carbon sinks, timber supply, and ecological services (Erdle and MacLean 1999). Outbreaks of spruce budworm (*Choristoneura fumiferana* Clem., hereafter SBW) are the dominant natural disturbance of balsam fir (*Abies balsamea* (L.) Mill.) and spruce (*Picea spp.*) forests in eastern North America (e.g., Morris 1963; MacLean 2016). During an outbreak in the 1970s–1980s, SBW caused defoliation covered ca. 50 million ha, with resulting losses of spruce-fir timber of 32–43 million m^3 $year^{-1}$ (Sterner and Davidson 1982). Understanding how defoliation varies across the landscape, as well as the underlying factors that shape these patterns, is essential for developing strategies to manage forests in ways that reduce impacts associated with outbreaks (MacLean et al. 2002; Hennigar et al. 2013).

Spatiotemporal patterns of SBW defoliation over large scales using aerial survey data have been described in several studies. In Ontario, from 1941–1996 three distinct outbreak zones were separated by two longitudinal corridors of lower defoliation severity (Candau et al. 1998). In Québec from 1965–1992, cluster analysis revealed 25 unique defoliation patterns that explained ~80% of the variation (Gray et al. 2000). For all of Canada from 1941–1998, Gray and MacKinnon (2006) described 27 defoliation patterns, which they grouped into seven severity classes ranging from "very mild" (<5 years of defoliation, average cumulative defoliation <50%) to "severe" and "very severe" (>25 years of defoliation, average cumulative defoliation >300%). Most recently, defoliation in Québec from 1938–2001 was reanalyzed by Cooke (2024), who showed that the number of derived clusters may be arbitrarily high, depending on the selection criteria used. Using 40 clusters, for example, identified behaviour that was "unique": cycling in the Ottawa valley at 24 years/cycle, as opposed to the 35-year cycle observed everywhere else (Cooke 2024). Finally, in in New Brunswick from 1965–1992, Zhao et al. (2014) defined 28

defoliation patterns, grouped into five SBW outbreak classes. In all of these studies, defoliation patterns differed in terms of duration, severity, and consistency, and were often found to be bi-modal, with several years of low defoliation separating high-severity "peaks" (e.g., Gray and MacKinnon 2006).

Several factors have been identified that significantly affect defoliation patterns. Because of SBW's relative specialization and feeding preferences, the availability of host species has a particularly strong impact. Balsam fir is typically more defoliated than spruce, with white spruce (*Picea glauca* (Moench) Voss), red spruce (*Picea rubens* Sarg.), and black spruce (*Picea mariana* [Mill.] B.S.P.) in mixed fir-spruce stands sustaining 72%, 41%, and 28% as much defoliation as balsam fir (Hennigar et al. 2008). This is consistent with the higher mortality rates observed in balsam fir than spruce species (e.g., MacLean 1980; Nealis and Régnière 2004). Forest hardwood content diminishes defoliation intensity, as stands with a higher proportion of non-host hardwoods may foster a greater abundance and diversity of natural enemies (i.e., parasitoids and predators) (Su et al. 1996; Zhang et al. 2018) or increase larval dispersal losses (Zhang et al. 2020) that reduces SBW populations. Insecticide spraying, if present in an area, is used to reduce defoliation in the treatment year (Fuentealba et al. 2015, 2023); it is prevalent in parts of eastern Canada and is important to account for in projecting effects of defoliation on forest growth and survival. Elevation may influence defoliation (Bouchard and Auger 2014), perhaps due to temperature differences or species composition variation with elevation. Temperature affects tree vigor and therefore its ability to tolerate defoliation, and higher mortality has been observed above 700m (e.g., Blais 1980; Witter 1985). Climate influences defoliation patterns (Candau and Fleming 2005, 2011; Gray 2013), and affects autocorrelation of defoliation spread (Bouchard and Auger 2014; Nenzén et al. 2018). Other factors, such as soil drainage, slope, and aspect appear to be either less important or inconsistent in terms of their

impact on defoliation patterns (MacLean and Ostaff 1989; Bergeron et al. 1995).

Although species composition, insecticide spraying, elevation, and climate all influence defoliation patterns, it can be difficult to distinguish their relative impacts from one another. Climate, stand, and site data, for example, are often spatially autocorrelated i.e., locations close to one another exhibit more similar values than those farther apart (Dormann et al. 2007). If autocorrelation is overlooked, the assumption of data independence of residuals may be violated, leading to false conclusions about the relative importance of different factors influencing ecological relationships. Spatial autocorrelation analyses showed that that 28–47% of plots had significantly clustered defoliation of trees within plots and a model including plot average defoliation and subject tree basal area explained 80% of the variance (Li et al. 2019). A regression tree was able to account for the spatial autocorrelation in defoliation frequency at all but the shortest (<30 km) distances, where stand age or species composition and SBW dispersal interact to overcome relationships with climate and forest characteristics (Candau and Fleming 2005). Fleming et al. (1999) observed that spatial autocorrelation waxed and waned through time as the SBW went through sawtooth-like subcycles, probably as a function of variable density-dependent dispersal. In survey data from New Brunswick, populations of second-instar larvae were spatially aggregated throughout the declining phase of a SBW outbreak cycle but became less so as densities decreased (Fleming et al. 1999). Ultimately, SBW defoliation is a function of number of SBW larvae and population processes, most notably dispersal that is most likely to explain time-varying spatial autocorrelation, but these may also be influenced by stand, site, and climate.

Here, we analyse spatiotemporal defoliation patterns occurring over an 11-year period on Gaspé Peninsula, Québec, beginning from 2012 when the outbreak was just starting to build up in the area. Our data were derived from a network of 99 sample plots in the central area of the

Gaspé Peninsula, with annual defoliation assessments from 2011–2021 using more than 9,500 branch samples and 28,000 ocular tree defoliation assessments (Donovan and MacLean 2024). These analyses extend past studies in several important ways. Whereas past studies tended to focus on defoliation patterns occurring during the peak to declining phases of outbreaks, our study may be the first to examine patterns during the early build-up phase of outbreak. Whereas past studies relied mainly on relatively crude aerial survey data to construct patterns, our analyses are based on precise branch-level data; aerial survey defoliation estimates in these plots corresponded with mean branch sample defoliation in only 43% of cases and ranged from only 14%–58% in individual years (Donovan and MacLean 2024). Past studies were all at a provincial or national scale, whereas our study area is only about 200km^2, but using precise defoliation data to determine smaller scale defoliation patterns. Moreover, because there was an ongoing foliage protection program in the area, we were also able to assess how periodic insecticide treatments influenced defoliation patterns, which reflects reality in most eastern Canada provinces.

Our study had three objectives. First, we used cluster analyses to classify plot-level patterns of annual balsam fir, white spruce, and black spruce cumulative defoliation from 2011–2021. Second, we assessed the occurrence of spatial autocorrelation in current-year balsam fir defoliation patterns among plots within and between stands. Finally, we quantified the relative importance of different factors, such as stand species composition, insecticide treatment history, site, and climate variables on balsam fir current and cumulative defoliation.

Methods

Study area and sample plot establishment

The study area was located in the Gaspé Peninsula, Québec, part of the Temiscouata-

Restigouche Forest Section of the Great Lakes-St. Lawrence Region (Rowe 1972) (Fig. 1). SBW defoliation was first detected in this region by annual aerial surveys in 2012 (MRNF 2021). Forests in the area are composed mainly of balsam fir and white birch (*Betula papyrifera* Marsh.) (Rowe 1972), with balsam fir and white spruce abundant at low elevations and black spruce common in poorly drained areas. The landscape has rolling topography with rivers creating narrow valleys and alluvial flats (Rowe 1972). Mean elevation is 365 metres (m), mean annual temperature ranges from 0–2.5°C, mean annual precipitation from 900–1100 millimetres, and the growing season lasts 150–160 days (Robitaille and Saucier 1998).

In 2014, 40 and 59 circular 0.04 ha sample plots were established in 28 stands northeast and southwest of the towns of Amqui and Causapscal, respectively (Fig.1). All plots contained balsam fir, white spruce, or black spruce (Supplementary Table S1); all Causapscal plots and most Amqui plots were dominated by balsam fir, but 6 Amqui plots were selected to represent hardwood-dominated or mixed hardwood-balsam fir (Zhang et al. 2018). Elevation of plots averaged 284 m (range 177–404 m). Due to timber harvesting over the next decade, 12 plots were lost, leaving 87 plots, averaging 165m apart, within 25 stands; there was an average of 3.5 plots per stand (range 1–6). Stands within the Amqui and Causapscal sites were within 4.3 km of each other; and there was 40 km separating the Amqui and Causapscal locations (Fig. 1). Therefore, we are examining defoliation at three scales: within stand, between stands, and between the Amqui and Causapscal locations.

Annual SBW defoliation measurements

Percent current-year defoliation was measured in each plot in August after larval feeding had finished by assessing shoots from one mid-crown branch sampled using pole pruners from each of a target of 15 trees per host species per plot per year (Donovan and MacLean 2024). Average height of dominant and co-dominant trees of the leading species in the stand (i.e.,

158 Lorey's mean height) ranged from 14.3m to 19.3m (Supplementary Table S1) and we usually
159 used 8–10 pole pruner sections (about 14–17 m) to sample branches, sometimes 11 sections (19
160 m) when required for the tallest trees. If 15 trees per host species were not present in a plot, we
161 sampled branches from all trees present; this occurred in 12% of balsam fir samples (where a
162 mean of 11 trees/plot were sampled), 43% of black spruce (mean 10 trees/plot sampled), and
163 66% of white spruce (mean 8 trees/plot sampled). The target sample sizes were based on
164 estimating mean stand defoliation with 90% confidence and ±10% error (MacLean and
165 MacKinnon 1998). Defoliation of current-, 1-, and 2-year-old foliage was measured on each of
166 25 randomly-selected shoots per branch, rated using seven percent defoliation classes (0, 1–20,
167 21–40, 41–60, 61–80, 81–99, 100%) (Fettes 1950). In 2014, the first year of sampling,
168 defoliation was estimated for older 2011, 2012, and 2013 foliage age-classes. Mean defoliation
169 per branch and foliage age-class was calculated using defoliation class mid-points. Mean
170 defoliation per host species per plot was calculated by weighting defoliation per tree by the basal
171 area of each sampled tree (Donovan and MacLean 2024). Mean cumulative defoliation per
172 species per plot over the 11-year period was calculated by summing current defoliation of that
173 species and plot for all years.

174 **Stand, site, and climate variables to be related to defoliation**

175 During plot establishment and again in 2018 and 2021, every tree ≥ 3 cm diameter at breast
176 height (DBH) was measured for species, DBH, height, height of base of live crown, and distance
177 and azimuth (degrees) from the plot centre. Heights and distances were measured with a Vertex
178 III and Transponder T3, Haglöf, Sweden. A total of 23 stand, site, or climate explanatory
179 variables was assembled for each plot (Table 1), based generally on the literature described in the
180 Introduction of factors thought to determine SBW defoliation levels, and were related to current-
181 year and cumulative defoliation. Seven stand explanatory variables included species composition

(basal area of balsam fir, white spruce, black spruce, hardwoods, and total basal area); annual aerial spraying of the biological insecticide *Bacillus thuringiensis* spp. *kurstaki* (Btk) against SBW (which began in 2015 and occurred in 11% of the samples, which henceforth we will term plot-years), determined using spatially referenced spray blocks provided by the Québec government. To be clear, the 87 plots were mostly sampled for 11 years each, but a few plots were harvested and sampled for only 6–8 years; this resulted in a total sample of 819 annual plot samples – i.e., 819 plot-years. Insecticide spraying occurred in a total of 87 plot-years, with 21 plots receiving at least 1 year of spraying: 6 plots received 1 or 2 years of spraying, and 15 plots received 5 or 6 years of spraying. SBW previous-year overwintering second-instar larvae (L2) populations were interpolated from the Québec government L2 sampling plot network, using the inverse distance weighting interpolation tool in ArcGIS Pro version 3.2.2 (ESRI, 2023) with a search neighbourhood of the L2 nearest estimates. Six site explanatory variables included elevation, aspect, and slope measured directly in each plot; soil nutrient/moisture quality class (poor, moderate, or rich soil nutrients and dry, moderate, or wet soil moisture), assigned based on a soil pit dug and vegetation indicator species sampled in each plot and a site classification system for the New Brunswick Kedgwick region (Zelazny et al. 1989), which is 25–32 and 60–66 km from the Causapscal and Amqui plots, and part of the same Temiscouata-Restigouche Forest Section (Rowe 1972) as our study area; and a depth-to-water index (Murphy et al. 2009) calculated from a Québec LiDAR-derived digital elevation model (MRNF 2016) and the Arc Hydro: Wetland Identification Model in ArcGIS Pro (Maidment 2002). Ten climate explanatory variables included cumulative degree days >5°C; summed monthly means per year of daily extreme minimum and maximum temperatures for spring, summer, and winter (April-May, June-July, November-March) and spring and summer precipitation (Table 1). These climatic periods and variables were based on SBW biology and life stages, such as spring emergence larval

survival, summer larval feeding, and overwintering survival. The BioSIM (v11) Weather Generator Editor (Régnière et al. 2017) was used to calculate 2011–2021 daily minimum and maximum temperatures (°C) and precipitation (mm) for each plot based on latitude, longitude, and elevation, using the four nearest weather stations, as recommended in the BioSIM manual.

Cluster analysis of defoliation patterns

Patterns of current and cumulative defoliation were grouped using the cluster analysis unsupervised learning technique, which assesses values by virtue of their similarity to each other and dissimilarity to other values (Everitt et al. 2011). Hierarchical cluster analysis used only plots with all 11 years (2011–2021) of defoliation measurements: 54 plots for balsam fir, 9 for white spruce, and 15 for black spruce. Yearly defoliation was standardized, centering means to zero and scaled to one standard deviation, which ensures equal importance is given to any defoliation year during clustering and is a common practice if variables have varying units and ranges (James et al. 2021). The "scale" function in the R statistical language (R Core Team 2023) was used and graphing was done in RStudio version 2023.12.1.402 (R Core Team 2023). We used the Euclidean distance matrix (James et al. 2021) computed using the "dist" function to measure distances between pairs of values, the "hclust" function and "Ward.D2" linkage method from the "stats" package (R Core Team 2023). The hclust function within R computes the actual hierarchical clustering, and the Ward.D2 method (Ward 1963) is one option for controlling how the algorithm creates clusters, minimizing within-cluster variance and helping to ensure data within each cluster are similar to each other. To select the optimum number of clusters that best described defoliation patterns, we examined three internal validation metrics: the total within-cluster sum of squares (TWCSS), Dunn index (DI), and average silhouette width (SW). The "clValid" and "factoextra" packages (Brock et al. 2008; Kassambara and Mundt 2020) were used to calculate validation metrics for visual comparison for a range of 1 to 20 potential clusters. The

optimum number of clusters was heuristically selected when increasing the number of clusters showed a negligible change based on averaging the three metrics.

Spatial autocorrelation of defoliation patterns within and between stands

Two spatial autocorrelation analyses were completed to characterize whether mean balsam fir current defoliation of plots was clustered, dispersed, or random. The global Moran's *I* index (Moran 1950) ranges from -1 to 1 and represents an overall measure of spatial autocorrelation based on testing a null hypothesis that the attribute being examined has a complete spatial randomness pattern among features for a study area. Accompanying p-values represent the probability that an observed pattern is random, and z-scores represent the standard deviations associated with a normal distribution. Global Moran's *I* analysis used the "Incremental Spatial Autocorrelation" tool in ArcGIS Pro 3.2.2 (ESRI, 2023), testing a range of distances from 100–600m in increments of 100m for within-stand, and 1000, 2500, 5000, 10,000, and 20,000m distances to examine between-stand defoliation clustering.

The second spatial autocorrelation analysis determined the Getis-Ord *Gi** statistic, which can help identify localized spatial clustering of neighbouring plots by identifying 'hot spot plots' (highly defoliated plots surrounded by other highly defoliated plots) and 'cold spot plots' (lightly defoliated plots surrounded by other lightly defoliated plots) (Getis and Ord 1992). *Gi** equates to the sum of the differences between individual plots and the mean of all plots representing a standard normal distribution z-score. When the local sum greatly differs from the expected local sum based on random chance, statistically significant z-score results are obtained. This analysis was conducted using the "Hot Spot Analysis" tool in ArcGIS Pro.

Mixed-effects modelling of stand, site, and climate effects on balsam fir defoliation

Differences in mean annual current defoliation among species were tested using Welch's analysis of variance followed by pairwise comparisons using the Games-Howell method. This

method accounted for unequal variances and sample sizes among species and was conducted using the "stats" and "rstatix" R packages (Kassambara 2023; R Core Team 2023).

We used generalized mixed-effects modelling (GLMM) for current defoliation (which is bounded between 0–100%) and linear mixed-effects modelling (LMM) for cumulative defoliation (which had a linear pattern year over year) to determine the effects of stand, site, and climate explanatory variables (Table 1). Two- and three-way interaction terms were included to test effects of significant and biologically relevant variable combinations on defoliation. GLMMs defined with a binomial distribution and logit link function are suitable when response variables are bounded percentage data (Zuur et al. 2009). Both GLMMs and LMMs enable correct inference when handling complex data that are hierarchical in nature, have non-independence, and include missing observations (Zuur et al. 2009). Models dealt with hierarchical and repeating observations, reducing spatiotemporal autocorrelation by defining random intercepts for sample plots nested within stands and crossing with year as the random effect structure. All suitable fixed-effect explanatory variables were standardized to have a mean of zero and scaled to one standard deviation, enabling easier interpretability of model estimates. Assumptions (e.g., residual homogeneity, linearity) were checked, and modelling used the "glmer" and "lmer" functions in the "lme4" package (Bates et al. 2015).

Explanatory variables were initially tested separately and ranked in importance based on parameter estimates, t-statistic (LMM) or z-statistic (GLMM), and p-value. Subsequent modelling based on maximum likelihood estimations started with the most significant variable and iteratively added (forward selection) the next most significant variable, resulting in the largest improvement of model goodness-of-fit (James et al. 2021; Zuur et al. 2009). At each model iteration adding an additional variable, analysis of variance likelihood ratio testing, Akaike Information Criterion (AIC), Bayesian Information Criterion (BIC), marginal R^2,

conditional R^2, and root mean squared error (RMSE) were evaluated; final models were identified based on the lowest BIC. Pearson's pairwise collinearity matrix (Supplementary Fig. S1) followed by iterative checks of variance inflation factors (VIFs) helped identify signs of multicollinearity; VIFs >10 were considered an issue (Dormann et al. 2013), and analyses ensured VIFs were <5 for selected variables. Final GLMM log-odds estimates were converted to probabilities to better understand the effects of fixed-effect variables on the response.

Results

Defoliation variability among species and plots

Annual current and cumulative defoliation for all plots combined by host species are presented as box plots in Fig. 2. Current defoliation increased each year from 2011 to 2015, reached a maximum in 2015 and 2017, and then was lower in at least some plots from 2018 to 2021 (Fig. 2a). Although there was wide variability among plots, demonstrated by the "length" of box plots in Fig. 2a, consistent trends among species were evident. "Sawtooth-like fluctuations" (sensu Royama 1984) were evident, with local peaks for white spruce and balsam fir in 2015, 2017, and 2020. The order of defoliation was always balsam fir > white spruce > black spruce (Fig. 2a). Mean defoliation of balsam fir was significantly greater than white spruce in 7 years (2011–2014 and 2016–2018) (letters above the x-axis in Fig. 2a). In the other 4 years, defoliation of white spruce was almost as high as balsam fir (Fig. 2a). In contrast, mean defoliation of black spruce was significantly lower than balsam fir in all years and lower than white spruce in 7 of 11 years (Fig. 2a). The highest mean current defoliation of black spruce in all plots was about 30%, compared to about 50% for white spruce and 70% for balsam fir. However, maximum current defoliation of individual plots was 100% for balsam fir, about 80% for white spruce, and 60% for black spruce (Fig. 2a).

Mean cumulative defoliation, calculated as the sum of current annual defoliation, gradually increased over the 11 years and reached nearly 500% for balsam fir, 350% for white spruce, and 150% for black spruce (Fig. 2b). These values can be interpreted as complete removal of the equivalent of about 5, 3.5, and 1.5 age-classes of foliage for the three species, respectively. Maximum cumulative defoliation among all plots over the 11 years was 650% for balsam fir, 400% for white spruce, and 200% for black spruce (Fig.2b).

Cumulative defoliation patterns of balsam fir and spruce

Cluster analysis divided the 54 plots with complete 2011–2021 balsam fir defoliation data into four clusters, with 9 to 20 plots per cluster (Fig. 3a). Clustering validation metrics led us to select four clusters, based mainly on SW but also TWCSS and DI metrics (Supplementary Fig. S2). Clusters 1 to 4, respectively, had mean cumulative defoliation of balsam fir after 11 years of 362%, 411%, 549%, and 615% (Fig. 3a). Three years earlier, in 2018, the four clusters had the same order of mean cumulative defoliation. Cluster 1 had the lowest cumulative defoliation and the highest frequency of insecticide spraying (29 plot-years, in 7 of the 11 years) (Fig. 3a). Cluster 2 also had a high frequency of insecticide spraying (24 plot-years, in 6 years). Cluster 3 was the most common pattern, and only had 7 plot-years of insecticide spraying. Cluster 4 had no insecticide spraying. Temporal patterns of cumulative defoliation were generally similar among clusters, except Clusters 1 and 2 had lower defoliation before 2015 and substantially lower defoliation due to insecticide spraying (Fig. 3a). Clusters 2 and 3 were the dominant defoliation patterns at the Causapscal site, whereas all four clusters were present at the Amqui site (Fig. 3a).

Although balsam fir was the dominant species (Supplementary Table S1), there were sufficient white spruce in five stands and black spruce in six stands to conduct cluster analyses on spruce (Fig. 3b, 3c). Most previous regional studies have combined defoliation patterns for fir

and spruce species. White spruce had four clusters, culminating in about 220%, 310%, 325%, and 400% mean cumulative defoliation, respectively (Fig. 3b). Defoliation in the three clusters for black spruce resulted in mean defoliation levels of about 120%, 150%, and 220% (Fig. 3c). Four of the seven spruce clusters resulted from plots in single stands. Four white spruce plots and four black spruce plots received aerial applications of Btk in 2–7 years (Fig. 3b, 3c).

Current annual defoliation patterns of balsam fir

Cluster analysis results were more complex for current defoliation (Fig. 4). We selected 10 clusters as optimal, based on diminishing returns when averaging the TWCSS, DI, and SW validation metrics for various numbers of clusters (Supplementary Fig. S2). In contrast to cumulative defoliation, current defoliation clusters tended to represent plots in only one or two stands, with only clusters 8 and 10 representing plots from 3 or 4 stands (Fig. 4). Insecticide spraying against SBW occurred in only 5 of the 10 clusters and coincided with years of low defoliation in some cases but not in others (Fig. 4). Although cumulative defoliation smoothly increased over time (Fig. 3), year-to-year fluctuations determined the current defoliation cluster results (Fig. 4). Plots in the most severe cumulative defoliation cluster 4 (Fig. 3a) were all in current defoliation clusters 9 or 10 (Fig. 4). Clusters 1, 2, and 5–7 represented plots from the Causapscal site, whereas clusters 3, 4, 8, and 9 had plots from both study sites, and cluster 10 contained only plots from the Amqui site (Fig. 4). Cluster 1 (stand 16) was late to the outbreak and was located somewhat distal from the others (Fig. 1). Defoliation in most clusters declined in 2016, but not in Cluster 3, which was noteworthy in having high hardwood content in stand 25 and high black spruce in stand 10 (Supplementary Table S1).

With few exceptions, the 2–5 plots within each stand had very similar balsam fir current defoliation patterns over time (Supplementary Fig. S3). Only two of the 24 stands (numbers 15 and 24) had plots in more than one current defoliation cluster (Fig. 4). This suggests that stand-

to-stand variability in current defoliation was much greater than plot-to-plot variability within stands, and sampling effort would be more productive with more individual stands than replicated plots within stands.

Spatial autocorrelation of balsam fir current defoliation within and between stands

Based on global Moran's *I* results, spatial clustering of balsam fir current defoliation within a given stand was statistically significant in all years and distances (Table 2). Moran's *I* was highest at 0.94 in 2016, the year in which defoliation decreased sharply, and lowest but still significant in 2012 at 0.41 (Table 2). Across the within-stand distances tested (100–600m), 100–300m often (71% of the time) had the highest Moran's *I* in any given year (Table 2), suggesting mean defoliation severity generally was similar at short distances among plots. At between-stand distances, plots were significantly clustered at 2500 and 5000m distances in all years, but Moran's *I* values were lower than within stands (Table 2). Defoliation was not significantly clustered for 2 of the 11 years at 5000m and for 5 years at distances of 10000 and 20000m (Table 2).

Both significant 'hot spot' (highly defoliated) and 'cold spot' (lightly defoliated) plots occurred (Fig. 5). The proportion of hot spot plots ranged from 7–25% among years (Table 3), generally with mean current defoliation >60%, whereas cold spot plots ranged from 6–25%, with mean current defoliation <50% (Fig. 5). Although current defoliation was significantly clustered in all years, it really occurred spatially at low or high defoliation levels, and 54–80% of plots (range among years) were not significantly clustered (Table 3; Fig. 5). Hot and cold spot plots did occur within the same stands in a given year, indicating that current defoliation was often spatially autocorrelated (mapped examples are shown in Supplementary Fig. S4).

Stand, site, and climate factors influencing SBW defoliation patterns

Results of forward-selection modelling of explanatory variables affecting balsam fir

cumulative and current defoliation are shown in Table 4. The LMM that we selected for balsam fir cumulative defoliation included five significant main effect variables: Sprayed, SuMinTp, SuMaxTp, HWba, and WSba, and interactions between L2branch*HWba, and L2branch*WSba (Model M4b; Table 4). Adding interaction terms of L2branch with HWba and WSba*L2branch slightly lowered AIC and BIC (Table 4), resulting in significant yet minor effects on cumulative defoliation (Fig. 6f and 6g). Fixed effects accounted for 9% of cumulative defoliation variation (marginal R^2), and random effects explained an additional 84% variation (conditional R^2; 2% for plots nested within stands, 7% for stands, and 83% for year variable) (Table 4).

Spraying insecticides resulted in a strong negative effect (Sprayed, -84.1; Table 5), reducing cumulative defoliation by 34–177% each year from 2015–2021 (Fig. 6a). Summed summer monthly minimum temperature had a weaker negative effect (SuMinTp, -19.3; Table 5); early in the outbreak (2011–2016), cumulative defoliation increased as SuMinTp increased, but later this shifted to a negative relationship (Fig 6b). Summed summer monthly maximum temperature showed a positive but inconsistent effect (SuMaxTp, 29.8; Table 5) on cumulative defoliation; positive in 4 years, negative in 2 years, and no relationship in 4 years (Fig. 6c). Main effects of hardwood (HWba, -17.1) and white spruce (WSba, -10.4) basal area both negatively affected defoliation (Table 5; Figs. 6d and 6e). The interaction of L2branch*HWba negatively (-15.2; Table 5) affected cumulative defoliation; for moderate SBW levels, 4 of 11 years were negative and 3 years positive, whereas 3 of 6 years having high SBW were negative (Fig. 6f). The interaction of L2branch*WSba was also negative (-8.5; Table 5) but inconsistent; for moderate SBW, 5 of 9 years were negative and 3 years positive, while for higher SBW levels, 4 of 6 years were negative (Fig. 6g).

The selected GLMM for balsam fir current defoliation included six significant main effect variables: Sprayed, L2branch, WiMaxTp, SuMaxTp, SuMinTp, HWba, and interactions of

Sprayed*SuMinTp, and L2branch*HWba (Model M5b, Table 4). The interaction term for HWba in most years indicated a stronger effect in reducing current defoliation at high L2 levels (Fig. 7g) and that current defoliation of sprayed plots decreased with SuMinTp but at low defoliation levels (Fig. 7f). The current defoliation model had a marginal R^2 of 0.19 and conditional R^2 of 0.54 (2% for plots, 8% for stands, and 90% for grouping variable year) (Table 4).

Annual spraying of insecticides had a strong negative effect on current defoliation (log-odds values are shown in Table 5), with mean current defoliation reduced by 11–60% due to spraying in 6 years (Fig. 7a). 2017 was the exception, with mean current defoliation 9% greater in sprayed than unsprayed plots (Fig. 7a). Overall, only 11% of the 819 plot-years analyzed were sprayed with insecticide, with spraying concentrated in specific stands or clusters from 2015 to 2021 (Figs. 3, 4, and S3). L2branch positively affected current defoliation, once mean defoliation exceeded 25% in 2013 (Fig. 7b). SuMinTp negatively but inconsistently affected current defoliation, with defoliation increasing with warmer summer minimum temperatures in 5 years, versus decreasing in 5 years (Fig. 7c). SuMaxTp also negatively but inconsistently affected current defoliation, negative in 5 years and positive in 5 years (Fig. 7d). WiMaxTp positively affected current defoliation in 7 of 11 years (Fig. 7e). The interaction of Sprayed*SuMinTp was inconsistently negative but indicated spraying reduced current defoliation at lower severities for 3 of 6 years from 2015–2021 (Fig. 7f). Finally, the interaction of L2branch*HWba showed a negative reduction of current defoliation. Defoliation decreased with increasing HWba in 4 of 9 years with moderate SBW and in 3 of 6 years with high SBW levels (Fig. 7g).

Discussion

Our study provides a unique examination of the spatiotemporal defoliation patterns that occur during the buildup of a SBW outbreak, as well as identifying some of the key factors

422 driving these trends. Cluster analysis of balsam fir current-year defoliation simplified patterns
423 into 10 clusters, reflecting varying annual fluctuations among years within plots and stands. In
424 contrast, cluster analysis of cumulative defoliation converged into only four patterns. This has
425 implications for simplifying determination of impacts of SBW outbreaks, since cumulative
426 defoliation is strongly related to growth reduction and tree survival (e.g., Erdle and MacLean
427 1999; Hennigar and MacLean 2010). For example, local sampling of SBW defoliation could be
428 used to infer one of the four cumulative defoliation patterns we observed, or other higher or
429 lower cumulative defoliation, and used as input into existing defoliation-based stand growth
430 models (e.g., Erdle and MacLean 1999) to determine tree growth reduction, mortality, and
431 volume yield using models or a decision-support system (e.g., MacLean et al. 2001, 2002).
432 Results showed that defoliation patterns can vary considerably within our small geographic study
433 area, in contrast to the large regional defoliation patterns described in previous studies (e.g.,
434 Candau et al. 1998; Gray and MacKinnon 2006; Zhao et al. 2014) and that defoliation differed
435 among host species that were combined in previous studies.

436 Tree host species significantly affected current and cumulative defoliation severities, with
437 balsam fir > white spruce > black spruce, as found in previous studies (Hennigar et al. 2008;
438 Bognounou et al. 2017). Defoliation of white spruce was closer to that of balsam fir during
439 severe outbreak years, as also noted by Hennigar and MacLean (2010), Fuentealba et al. (2019),
440 and Bauce et al. (2024).

441 In any given year, within-stand spatial autocorrelation of balsam fir current defoliation was
442 significant when the severity of defoliation was light or severe but generally not when it was
443 moderate. This is probably a function of effects of SBW dispersal and high larval survival
444 driving population eruptions. When a major moth influx occurs, high SBW populations occur on
445 most trees or plots and result in similarly high (severe) defoliation in the area. When populations

are low, resulting in light defoliation, SBW only occurs close to oviposition sites on individual trees, so plots in an area have similarly light defoliation.

Balsam fir is the primary host for SBW due to the phenology synchronization between diapause emergence and bud flush during spring (Nealis and Régnière 2004), and possibly also due to white spruce having superior defensive chemicals (e.g., Delvas et al. 2011). In the years with highest balsam fir defoliation (2015, 2019–2021), white spruce had levels of defoliation approaching that of balsam fir. Bognounou et al. (2017) referred to this as associational susceptibility, where secondary hosts can temporarily become more susceptible from an influx of SBW populations, optimal climate perturbations, or primary resource depletion leading to spillover to secondary hosts. Our data also showed evidence of an associational resistance interaction between black spruce and balsam fir, similar to Bognounou et al. (2017). Black spruce was common throughout the Causapscal site and had low defoliation levels throughout the years sampled, even when balsam fir in the same stands sustained severe defoliation.

Our cluster analysis of defoliation patterns was unique compared to previous studies because it was based on precise branch defoliation data (Donovan and MacLean 2024), and the spatial scale focused on patterns within and between stands for a small part of the SBW range. In contrast, previous studies used less precise aerial survey data (Donovan and MacLean 2024) covering provincial or national scales (Candau et al. 1998; Gray and MacKinnon 2006; Zhao et al. 2014). Even at these different spatial scales, there were similarities in results. Clusters for current annual defoliation consistently resulted in various distinctive “up-and-down, sawtooth” patterns, whereas cumulative defoliation patterns were categorized by only a few groups (Gray and MacKinnon 2006; Zhao et al. 2014). Such similarities across temporal (i.e., different outbreaks) and spatial scales (i.e., different locations) provide support for use of cumulative defoliation scenarios in analyses of impacts using a decision-support framework (e.g., MacLean

et al. 2002). Although our defoliation patterns were from a small ~200km^2 area, results showed that 10 current annual defoliation patterns converged over time into only four cumulative defoliation patterns. Local SBW defoliation patterns derived from aerial surveys or satellite imagery can be used to assign these of other cumulative defoliation patterns to specific stands/forest and used as input into defoliation-based stand growth models (e.g., Erdle and MacLean 1999) to predict growth reduction, mortality, and guide harvest replanning, salvage, and insecticide prioritization to minimize losses (e.g., MacLean et al. 2001, 2002; Hennigar and MacLean 2010). Cluster analysis of defoliation patterns also showed the strong effect of aerial spraying of insecticides in reducing defoliation, which occurred only in 11% of the plot-years, confirming their effectiveness in forest protection (Fuentealba et al. 2015).

Balsam fir current defoliation patterns showed consistent synchrony within and between nearby stands based on spatial autocorrelation analysis. Many studies of forest insects link spatial autocorrelation at different scales to the Moran effect (Peltonen et al. 2002; Royama 2005). Population synchrony is driven by favourable spatially autocorrelated climate conditions and insect dispersal capabilities (Nenzén et al. 2018; Larroque et al. 2019). An essential aspect of climate effects on SBW dynamics relates to temperature sensitivity of all life stages (Pureswaran et al. 2015). Our analysis identified SuMinTp, SuMaxTp, and WiMaxTp as having positive and negative effects on observed defoliation, indicating that climatic differences over multiple years may play a significant role in defoliation differences.

Our hot and cold spot analysis indicated that within-stand spatial autocorrelation occurred at both light and severe defoliation levels. This suggests that multiple fine-scale interactions at the stand level likely support or counteract the broad-scale dispersal and climate mechanisms leading to localized SBW population fluctuations. There was generally a high proportion of plots showing significant clustering at both defoliation >80% and <~40%, but these thresholds varied

among years, especially for 2017. The hot and cold spot analysis essentially showed that defoliation of plots within a stand or in nearby stands tend to be clustered when defoliation was high and when it was low, but not intermediate. This might reflect effects of dispersal-driven sawtooth defoliation patterns but also high larval survival resulting in high defoliation, or the opposite for low defoliation level cold spots. In a previous study using a subset of our data, Li et al. (2019) found that spatially clustered defoliation also occurred among trees within plots, usually under high mean plot defoliation. Density-dependent regulation of SBW interacting with natural enemies (e.g., parasitoids, diseases, and predators) (Royama 1984; Bouchard et al. 2018) can contribute to both within-plot and local between-plot spatial clustering of defoliation.

Our mixed effect modelling strategy used forward selection methods and checking model goodness-of-fit and variance explained. Some simpler models performed almost as good as our final selected models. Careful consideration was given to additional main effects and interaction terms and how increasing model complexity helped explain variability in defoliation. For example, including the interaction of SBW L2branch*HWba significantly improved model goodness-of-fit but resulted in a marginal reduction in overall error, and a slight decrease in variance explained for current defoliation. In the context of SBW population dynamics, this relationship is an important mechanism due to increased natural enemy abundance and diversity with increased hardwood composition resulting in lower SBW populations and defoliation (Su et al. 1996; Zhang et al. 2018). The interaction of SBW L2branch*WSba is also relevant since white spruce offers adequate survival for SBW populations compared to balsam fir but is prone to less defoliation due to spruce's increased ability to produce numerous shoots (Nealis and Régnière 2004). However, from a management standpoint, insecticide spraying, L2 population level, and species composition can be used to estimate defoliation patterns.

Although our models of current and cumulative defoliation were significant, there were large differences between marginal R^2, which explains the variance for only fixed effects, and conditional R^2, which explains model variance for both fixed and random effects. The "Year" variable random effects explained a lot of the model variability and indicated that previous year defoliation was important to subsequent year defoliation, due to temporal autocorrelation.

Aerial spraying of insecticides had the strongest effect of any factors in reducing balsam fir current and cumulative defoliation. Spraying insecticides is an effective protective strategy for keeping host trees alive and reducing defoliation severity (Fuentealba et al. 2015, 2023). This effect was also evident in our cluster analysis of defoliation patterns as lower severity patterns were associated with more frequent insecticide spraying. Number of SBW L2 had a positive effect, causing increases in current defoliation, as would be expected. Number of SBW L2 (overwintering) are used as the threshold for triggering an early intervention insecticide use strategy against SBW (Johns et al. 2019; MacLean et al. 2019), which aims to minimize defoliation by detecting and treating localized rising SBW populations and also under a foliage protection strategy (Fuentealba et al. 2023).

Even though it is a cold-adapted species (Pureswaran et al. 2015), SBW overwintering survival is negatively influenced by extreme cold conditions, with a combination of temperature and exposure durations required to kill half of the population (LTT_{50}) of 11.4 hours at -39°C (Delisle et al. 2022). Although SBW larvae can withstand very low temperatures in winter, they are vulnerable to cold spells during early diapause or post-diapause development (Delisle et al. 2022). Extreme winter warming can also deplete SBW larval energy reserves, resulting in immediate or delayed mortality (Han and Bauce 1998; Moise et al. 2024). The threshold temperature triggering post-diapause development is thought to be near 2.5–5.5˚C (Bean 1961; Miller et al. 1971), and temperatures near this threshold may be one reason for higher mortality

during spring post-diapause development (Han and Bauce 1998). Overwintering survival is further complicated by host species selected by SBW (Berthiaume et al. 2020; Moise et al. 2023). Winter temperature fluctuations and timing are critical, and acute warming periods during early diapause reduce survival in contrast to warming periods later in diapause (Moise et al. 2024). Our results suggest that WiMaxTp was within the threshold range since there was a positive effect on current defoliation patterns. Interestingly, during 2021, we observed an unseasonably warmer winter than in previous years, which caused a negative effect on defoliation patterns. Candau and Fleming (2005, 2011) also found that warmer winter minimum and maximum temperatures were associated with higher defoliation frequency.

SuMinTp and SuMaxTp were significant factors, but their effects on defoliation patterns were inconsistent between years. Warmer SuMinTp negatively affected current and cumulative defoliation. An interaction between spraying and SuMinTp negatively affected current defoliation, which might reflect less effective spraying or operational issues achieving optimal timing under cold temperatures. However, it is important to recognize that we used coarse seasonal climatic measures (e.g., seasonal annual minimum and maximum temperatures) over 11 years, so any relationships with insecticide efficacy or SBW population dynamics are speculative. Warmer SuMaxTp negatively affected current defoliation and positively affected cumulative defoliation. Several previous studies have found somewhat similar results. Gray (2013) found that higher SuMinTp and SuMaxTp resulted in longer but less severe outbreaks, with the mechanism hypothesized to be potential disruption to natural enemies' survival dynamics along with reduced SBW feeding rates (Bellemin-Noël et al. 2021). Blais (1958) and Régnière et al. (2012) observed that cooler summer temperatures contributed to slower SBW larval development and reduced survival. Both Candau and Fleming (2011) and Nenzén et al. (2018) conducted SBW outbreak projections, finding that summer temperatures along with

spring and winter temperatures were important. Increasing SuMaxTp up to a threshold of 18˚C resulted in the increased probability of severe defoliation for a SBW outbreak in Newfoundland (Zhang et al. 2023). Such results among literature and our study suggest there are multiple compounding factors related to temperature causing complexity of SBW feeding and survival during the summer period.

Conclusions

Host tree species strongly influenced SBW current and cumulative defoliation over an 11-year period, with balsam fir > white spruce > black spruce, similar to results from most previous studies. On average, balsam fir defoliation was 13% greater than white spruce and 29% greater than black spruce.

Cumulative defoliation tended to converge into a few general patterns, which cluster analysis placed into 4, 4, and 3 patterns for balsam fir, white spruce, and black spruce, respectively. In contrast, balsam fir current defoliation had much more year-to-year fluctuation, which cluster analysis grouped into 10 patterns. The ability to aggregate cumulative defoliation patterns can assist in building accurate geo-referenced defoliation-based growth reduction estimates based on stand characteristics and stand-to-stand defoliation spread and synchronization.

Spatial autocorrelation of balsam fir current defoliation within and between stands was significant, especially at low and high defoliation severities, and gradually weakened when distances exceeded >2500m. From an outbreak monitoring viewpoint, future ground-based defoliation assessments would be more efficient by deploying 1–3 sample plots per stand, to increase the number of assessed stands.

Stand species composition and insecticide treatment were the primary determinants of

589 defoliation patterns, with climate showing minor effects and site no effects. Significant factors
590 related to balsam fir current and cumulative defoliation patterns were Sprayed, L2branch,
591 SuMinTp, SuMaxTp, WiMaxTp, and interactions L2branch*HWba, and Sprayed*SuMinTp.
592 Spray and L2branch were expected variables included in final models, since spraying reduces
593 SBW populations and defoliation, and overwintering L2branch estimates are a proxy for the
594 following year feeding larval SBW population. SuMinTp had a negative effect on defoliation but
595 was inconsistent among years; SuMaxTp had negative and positive effects on current and
596 cumulative defoliation, respectively; and WiMaxTp had a positive effect on current and
597 cumulative defoliation patterns. Each interaction term had a negative effect on current and
598 cumulative defoliation, but significance was marginal and inconsistent across years. Such
599 relationships, which are known to influence SBW larval development, phenology, overwintering
600 mortality, and host-natural enemy interactions, suggest that temperature can also significantly
601 influence defoliation patterns over a long period within a relatively small local area of <200km^2.
602

603 **CRediT author contribution statement**

604 **Shawn D. Donovan:** Project conceptualization, Data curation, Formal analysis, Visualization
605 Writing – original draft, review & editing. **David A. MacLean:** Project conceptualization,
606 Supervision, Administration and funding acquisition, Writing – original draft, review & editing.
607 **Chris Hennigar:** Writing – review & editing. **Rob C. Johns:** Writing – review & editing. **Yun**
608 **Zhang:** Writing – review & editing.

609 **Declaration of Competing Interest**

610 The authors declare that they have no known competing financial interests or personal
611 relationships that could have appeared to influence the work reported in this paper.

612 **Acknowledgments**

This research was funded by the Atlantic Canada Opportunities Agency, Natural Resources Canada, Government of New Brunswick, and forest industry in New Brunswick under the Early Intervention Strategy Against Spruce Budworm program. Oversight was provided by the Healthy Forest Partnership, a consortium of researchers, landowners, forestry companies, governments, and forest protection experts in Atlantic Canada. We thank the Québec Ministère des Forêts de la Faune et des Parcs for permission to use their SBW L2 population data. Special thanks to all field technicians who assisted in the sample plot data collections. We appreciate constructive comments provided by three anonymous reviewers, which improved the paper.

Data Availability

Data generated or analyzed during this study are available from the corresponding author upon reasonable request.

References

Bates, D., Maechler, M., Bolker, B., and Walker, S. 2015. Fitting linear mixed-effects models using lme4. J. Stat. Softw. **67**(1): 1–48.

Bauce, É., Dupont, A., Hébert, C., Berthiaume, R., Quezada-García, R., and Fuentealba, A. 2024. Biennial aerial application of *Bacillus thuringiensis* Berliner var. *kurstaki* is the most cost-effective approach of protection against spruce budworm (*Choristoneura fumiferana* [Clemens]). Ann. For. Sci. **81:40**. doi:10.1186/s13595-024-01260-9.

Bean, J.L. 1961. Predicting emergence of second-instar spruce budworm larvae from hibernation under field conditions in Minnesota. Ann. Entomol. Soc. Am. **54**(2): 175–177. doi:10.1093/aesa/54.2.175.

Bellemin-Noël, B., Bourassa, S., Despland, E., De Grandpré, L., and Pureswaran, D.S. 2021. Improved performance of the eastern spruce budworm on black spruce as warming

637 temperatures disrupt phenological defences. Glob. Chang. Biol. **27**: 3358–3366.
638 doi:10.1111/gcb.15643.
639 Bergeron, Y., Leduc, A., Morin, H., and Joyal, C. 1995. Balsam fir mortality following the last
640 spruce budworm outbreak in northwestern Quebec. Can. J. For. Res. **25**: 1375–1384.
641 Berthiaume, R., Hébert, C., Charest, M., Dupont, A., and Bauce, É. 2020. Host tree species
642 affects spruce budworm winter survival. Environ. Entomol. **49**(2): 496–501.
643 doi:10.1093/EE/NVAA020.
644 Blais, J.R. 1958. Effects of defoliation by spruce budworm (*Choristoneura fumiferana* Clem.) on
645 radial growth at breast height of balsam fir (*Abies balsamea* (L.) Mill.) and white spruce
646 (*Picea glauca* (Moench) Voss.). For. Chron. **34**(1): 39–47. doi:10.5558/tfc34039-1.
647 Blais, J.R. 1980. Condition du sapin et de l'épinette blanche dans la région du parc des
648 Laurentides en 1979 face à l'épidémie de la tordeuse et prévision des pertes. Can. For.
649 Serv., Laurentian Forestry Centre, Quebec, QC. Inf. Rep. LAU-X-43.
650 Bognounou, F., De Grandprè, L., Pureswaran, D.S., and Kneeshaw, D. 2017. Temporal variation
651 in plant neighborhood effects on the defoliation of primary and secondary hosts by an
652 insect pest. Ecosphere **8**(3): e01759. doi:10.1002/ecs2.1759.
653 Bouchard, M., and Auger, I. 2014. Influence of environmental factors and spatio-temporal
654 covariates during the initial development of a spruce budworm outbreak. Landsc. Ecol. **29**:
655 111–126. doi:10.1007/s10980-013-9966-x.
656 Bouchard, M., Martel, V., Régnière, J., Therrien, P., and Correia, D.L.P. 2018. Do natural
657 enemies explain fluctuations in low-density spruce budworm populations? Ecology **99**(9):
658 2047–2057. doi:10.1002/ecy.2417.
659 Brock, G., Pihur, V., Datta, S., and Datta, S. 2008. ClValid: An R package for cluster validation.
660 J. Stat. Softw. **25**(4): 1–22. doi:10.18637/jss.v025.i04.

661 Candau, J.-N., and Fleming, R.A. 2005. Landscape-scale spatial distribution of spruce budworm
662 defoliation in relation to bioclimatic conditions. Can. J. For. Res. **35**: 2218–2232.
663 doi:10.1139/x05-078.
664 Candau, J.-N., and Fleming, R.A. 2011. Forecasting the response of spruce budworm defoliation
665 to climate change in Ontario. Can. J. For. Res. **41**: 1948–1960. doi:10.1139/x11-134.
666 Candau, J.-N., Fleming, R.A., and Hopkin, A. 1998. Spatiotemporal patterns of large-scale
667 defoliation caused by the spruce budworm in Ontario since 1941. Can. J. For. Res. **28**:
668 1733–1741. doi:10.1139/x98-164.
669 Cooke, B.J. 2024. On the characterization of patterning in spruce budworm time-series data.
670 Can. J. For. Res. **54**: 1183–1197. doi:10.1139/cjfr-2024-0040.
671 Delisle, J., Bernier-Cardou, M., and Labrecque, A. 2022. Cold tolerance and winter survival of
672 seasonally-acclimatised second-instar larvae of the spruce budworm, *Choristoneura*
673 *fumiferana*. Ecol. Entomol. **47**(4): 553–565. doi:10.1111/een.13140.
674 Delvas, N., Bauce, É., Labbé, C., Ollevier, T., and Bélanger, R. 2011. Phenolic compounds that
675 confer resistance to spruce budworm. Entomol. Exp. Appl. **141**: 35–44.
676 doi:10.1111/j.1570-7458.2011.01161.x.
677 Donovan, S., and MacLean, D.A. 2024. Evaluation of branch sampling, ocular assessments, and
678 aerial surveys for estimating spruce budworm defoliation. Can. J. For. Res. **54**: 725–740.
679 doi:10.1139/cjfr-2023-0240.
680 Dormann, C.F., Elith, J., Bacher, S., Buchmann, C., Carl, G., Carré, G., Marquéz, J.R.G.,
681 Gruber, B., Lafourcade, B., Leitão, P.J., Münkemüller, T., Mcclean, C., Osborne, P.E.,
682 Reineking, B., Schröder, B., Skidmore, A.K., Zurell, D., and Lautenbach, S. 2013.
683 Collinearity: a review of methods to deal with it and a simulation study evaluating their
684 performance. Ecography. **36**: 27–46. doi:10.1111/j.1600-0587.2012.07348.x.

685 Dormann, C.F., McPherson, J.M., Araújo, M.B., Bivand, R., Bolliger, J., Carl, G., Davies, R.G.,
686 Hirzel, A., Jetz, W., Daniel Kissling, W., Kühn, I., Ohlemüller, R., Peres-Neto, P.R.,
687 Reineking, B., Schröder, B., Schurr, F.M., and Wilson, R. 2007. Methods to account for
688 spatial autocorrelation in the analysis of species distributional data: a review. Ecography.
689 **30**: 609–628. doi:10.1111/j.2007.0906-7590.05171.x.
690 Environment Systems Research Institute (ESRI). 2023. ArcGIS Pro: Version 3.2.2. Redlands,
691 CA, USA. Redlands, CA.
692 Erdle, T.A., and MacLean, D.A. 1999. Stand growth model calibration for use in forest pest
693 impact assessment. For. Chron. **75**: 141–152.
694 Everitt, B.S., Landau, S., Leese, M., and Stahl, D. 2011. Cluster analysis. 5th edition. *In* Wiley
695 Series in Probability and Statistics. Wiley, Chichester, West Sussex, U.K.
696 Fettes, J.J. 1950. Investigations of sampling techniques for population studies of the spruce
697 budworm on balsam fir in Ontario. Forest Insect Laboratory, Sault Ste. Marie, Ont., Ann.
698 Tech. Rep. 4. pp. 163–401.
699 Fleming, R.A., Lyons, D.B., and Candau, J.N. 1999. Spatial transmutation and its consequences
700 in spatially upscaling models of spruce budworm population dynamics. Can. J. Remote
701 Sens. **25**: 388–402. doi:10.1080/07038992.1999.10874738.
702 Fuentealba, A., Bauce, É., and Dupont, A. 2015. *Bacillus thuringiensis* efficacy in reducing
703 spruce budworm damage as affected by host tree species. J. Pest Sci. **88**: 593–603.
704 doi:10.1007/s10340-014-0629-8.
705 Fuentealba, A., Dupont, A., Hébert, C., Berthiaume, R., Quezada-García, R., and Bauce, É.
706 2019. Comparing the efficacy of various aerial spraying scenarios using *Bacillus*
707 *thuringiensis* to protect trees from spruce budworm defoliation. For. Ecol. Manage. **432**:
708 1013–1021. doi:10.1016/j.foreco.2018.10.034.

709 Fuentealba, A., Pelletier-Beaulieu, É., Dupont, A., Hébert, C., Berthiaume, R., and Bauce, É.
710 2023. Optimizing *Bacillus thuringiensis* (Btk) aerial spray prescriptions in mixed balsam
711 fir-white spruce stands against the eastern spruce budworm. Forests **14**: 1289.
712 doi:10.3390/f14071289.
713 Getis, A., and Ord, J.K. 1992. The analysis of spatial autocorrelation in biological variables.
714 Geogr. Anal. **24**: 189–206.
715 Gray, D.R. 2013. The influence of forest composition and climate on outbreak characteristics of
716 the spruce budworm in eastern Canada. Can. J. For. Res. **43**: 1181–1195. doi:10.1139/cjfr-
717 2013-0240.
718 Gray, D.R., and MacKinnon, W.E. 2006. Outbreak patterns of the spruce budworm in Canada.
719 For. Chron. **82**: 550–561.
720 Gray, D.R., Regniere, J., and Boulet, B. 2000. Analysis and use of historical patterns of spruce
721 budworm defoliation to forecast outbreak patterns in Quebec. For. Ecol. Manage. **127**:
722 217–231.
723 Han, E.R.N., and Bauce, E. 1998. Timing of diapause initiation, metabolic changes and
724 overwintering survival of the spruce budworm, *Choristoneura fumiferana*. Ecol. Entomol.
725 **23**(2): 160–167. doi:10.1046/j.1365-2311.1998.00111.x.
726 Hennigar, C.R., and MacLean, D.A. 2010. Spruce budworm and management effects on forest
727 and wood product carbon for an intensively managed forest. Can. J. For. Res. **40**(9): 1736–
728 1750. doi:10.1139/X10-104.
729 Hennigar, C.R., Erdle, T.A., Gullison, J.J., and MacLean, D.A. 2013. Re-examining wood supply
730 in light of future spruce budworm outbreaks: a case study in New Brunswick. For. Chron.
731 **89**: 42–53. doi:10.5558/tfc2013-010.
732 Hennigar, C.R., MacLean, D.A., Quiring, D.T., and Kershaw, J.A. 2008. Differences in spruce

733 budworm defoliation among balsam fir and white, red, and black spruce. For. Sci. **54**(2):
734 158–166.
735 James, G., Witten, D., Hastie, T., and Tibshirani, R. 2021. An introduction to statistical learning:
736 with applications in R. 2nd edition. Springer texts in statistics. Springer.
737 Johns, R.C., Bowden, J.J., Carleton, D.R., Cooke, B.J., Edwards, S., Emilson, E.J.S., James,
738 P.M.A., Kneeshaw, D., and MacLean, D.A. 2019. A conceptual framework for the spruce
739 budworm early intervention strategy: can outbreaks be stopped? Forests **10**(910).
740 Kassambara, A. 2023. rstatix: pipe-friendly framework for basic statistical tests. R package
741 version 0.7.2. Available from https://cran.r-project.org/package=rstatix.
742 Kassambara, A., and Mundt, F. 2020. factoextra: extract and visualize the results of multivariate
743 data analyses. R package version 1.0.7. https://CRAN.R-project.org/package=factoextra.
744 Available from https://cran.r-project.org/package=factoextra.
745 Larroque, J., Legault, S., Johns, R., Lumley, L., Cusson, M., Renaut, S., Levesque, R.C., and
746 James, P.M.A. 2019. Temporal variation in spatial genetic structure during population
747 outbreaks: distinguishing among different potential drivers of spatial synchrony. Evol.
748 Appl. **12**: 1931–1945. doi:10.1111/eva.12852.
749 Li, M., MacLean, D.A., Hennigar, C.R., and Ogilvie, J. 2019. Spatial-temporal patterns of spruce
750 budworm defoliation within plots in Québec. Forests **10**: 232. doi:10.3390/f10030232.
751 MacLean, D.A. 1980. Vulnerability of fir-spruce stands during uncontrolled spruce budworm
752 outbreaks: a review and discussion. For. Chron. **56**: 213–221.
753 MacLean, D.A. 2016. Impacts of insect outbreaks on tree mortality, productivity, and stand
754 development. Can. Entomol. **148**: S138–S159. doi:10.4039/tce.2015.24.
755 MacLean, D.A., Amirault, P., Amos-Binks, L., Carleton, D., Hennigar, C., Johns, R., and
756 Régnière, J. 2019. Positive results of an early intervention strategy to suppress a spruce

budworm outbreak after five years of trials. Forests **10**: 448. doi:10.3390/f10050448.

MacLean, D.A., Beaton, K.P., Porter, K.B., MacKinnon, W.E., and Budd, M.G. 2002. Potential wood supply losses to spruce budworm in New Brunswick estimated using the Spruce Budworm Decision Support System. For. Chron. **78**(5): 739–750. doi:10.5558/tfc78739-5.

MacLean, D.A., Erdle, T.A., MacKinnon, W.E., Porter, K.B., Beaton, K.P., Cormier, G., Morehouse, S., and Budd, M. 2001. The Spruce Budworm Decision Support System: forest protection planning to sustain long-term wood supply. Can. J. For. Res. **31**: 1742–1757. doi:10.1139/cjfr-31-10-1742.

MacLean, D.A., and MacKinnon, W.E. 1998. Sample sizes required to estimate defoliation of spruce and balsam fir caused by spruce budworm accurately. North. J. Appl. For. **15**: 135–140.

MacLean, D.A., and Ostaff, D.P. 1989. Patterns of balsam fir mortality caused by an uncontrolled spruce budworm outbreak. Can. J. For. Res. **19**: 1087–1095.

Maidment, D.R. 2002. Arc Hydro: GIS for Water Resources. *Edited By* D.R. Maidemnt. Redlands, Calif: ESRI Press.

Miller, C.A., Eidt, D.C., and McDougall, G.A. 1971. Predicting spruce budworm development. Canadian Forest Service Bi-monthly Research Notes. **27**: 33-34.

Ministère des Ressources Naturelles et des Forêts (MRNF). 2016. LiDAR - Modèles numériques (terrain, canopée, pente), [Jeu de données], dans Données Québec, mis à jour le 16 juillet 2024. https://www.donneesquebec.ca/recherche/dataset/produits-derives-de-base-du-lidar.

Ministère des Ressources Naturelles et des Forêts (MRNF). 2021. Aires infestées par la tordeuse des bourgeons de l'épinette au Québec en 2021, Québec, gouvernement du Québec, Direction de la protection des forêts, 22 p.

Moise, E.R.D., Bowden, J.J., and Stastny, M. 2023. Suboptimal host tree benefits the

781 overwintering of a destructive forest insect pest. Basic Appl. Ecol. **71**: 72–84.
782 doi:10.1016/j.baae.2023.05.005.
783 Moise, E.R.D., Warren, J., and Bowden, J.J. 2024. Impacts of winter warming events on spruce
784 budworm: the importance of timing. J. Insect Sci. **24**(2): 17. doi:10.1093/jisesa/ieae037.
785 Moran, P.A.P. 1950. Notes on continuous stochastic phenomena. Biometrika **37**: 17–23.
786 Morris, R.F. 1963. The dynamics of epidemic spruce budworm populations. Entomological
787 Society of Canada Memoir 31.
788 Murphy, P.N.C., Ogilvie, J., and Arp, P. 2009. Topographic modelling of soil moisture
789 conditions: a comparison and verification of two models. Eur. J. Soil Sci. **60**: 94–109.
790 doi:10.1111/j.1365-2389.2008.01094.x.
791 Nealis, V.G., and Régnière, J. 2004. Insect-host relationships influencing disturbance by the
792 spruce budworm in a boreal mixedwood forest. Can. J. For. Res. **34**: 1870–1882.
793 doi:10.1139/X04-061.
794 Nenzén, H.K., Peres-Neto, P., and Gravel, D. 2018. More than Moran: coupling statistical and
795 simulation models to understand how defoliation spread and weather variation drive insect
796 outbreak dynamics. Can. J. For. Res. **48**: 255–264. doi:10.1139/cjfr-2016-0396.
797 Peltonen, M., Liebhold, A.M., Bjornstad, O.N., and Williams, D.W. 2002. Spatial synchrony in
798 forest insect outbreaks: roles of regional stochasticity and dispersal. Ecology **83**(11): 3120–
799 3129.
800 Pureswaran, D.S., De Grandpré, L., Pare, D., Taylor, A., Barrette, M., Morin, H., Regniere, J.,
801 and Kneeshaw, D.D. 2015. Climate-induced changes in host tree-insect phenology may
802 drive ecological state-shift in boreal forests. Ecology **96**(6): 1480–1491. doi:10.1890/07-
803 1861.1.
804 R Core Team. 2023. R: A language and environment for statistical computing. R Foundation for

805 Statistical Computing, Vienna, Austria. URL https://www.R-project.org/.
806 Régnière, J., Saint-Amant, R., Béchard, A., and Moutaoufik, A. 2017. BioSIM 11 User's
807 Manual. Canadian Forest Service, Laurentian Forestry Centre, Québec. Inf. Rep. LAU-X-
808 137. 67p.
809 Régnière, J., St-Amant, R., and Duval, P. 2012. Predicting insect distributions under climate
810 change from physiological responses: spruce budworm as an example. Biol. Invasions **14**:
811 1571–1586. doi:10.1007/s10530-010-9918-1.
812 Robitaille, A., and Saucier, J.P. 1998. Paysages régionaux du Québec méridional. Ministère des
813 Ressources Naturelles du Québec. Publication du Québec, Québec.
814 Rowe, J.S. 1972. Forest regions of Canada. Canadian Forestry Service. Ottawa, Canada.
815 Publication 1300.
816 Royama, T. 1984. Population dynamics of the spruce budworm Choristoneura fumiferana. Ecol.
817 Monogr. **54**(4): 429–462.
818 Royama, T. 2005. Moran effect on nonlinear population processes. Ecol. Monogr. **75**(2): 277–
819 293.
820 Sterner, T.E., and Davidson, A.G. 1982. Forest insect and disease conditions in Canada 1981.
821 Canadian Forest Service, Ottawa, ON.
822 Su, Q., MacLean, D.A., and Needham, T.D. 1996. The influence of hardwood content on balsam
823 fir defoliation by spruce budworm. Can. J. For. Res. **26**: 1620–1628.
824 Ward, J.H. 1963. Hierarchical grouping to optimize an objective function. J. Am. Stat. Assoc.
825 **58**(301): 236–244.
826 Witter, J.A. 1985. Characteristics of susceptible/vulnerable stands. pp. 354–355. In Recent
827 Advances in Spruce Budworms Research. Edited by Sanders, C.J., Stark, R. W., Mullins,
828 E.J., and Murphy, J.), Proc. CANUSA Spruce Budworms Research Symposium, 16–20

Sept. 1984, Bangor, ME. Can. For. Serv., Ottawa, ON.

Zelazny, V.F., Ng, T.T.M., Hayter, M.G., Bowling, C.L., and Bewick, D.A. 1989. Field guide to forest site classification in New Brunswick. Harvey-Harcourt-Fundy site regions. New Brunswick Department of Natual Resources and Energy, Fredericton.

Zhang, B., Leroux, S.J., Bowden, J.J., Hargan, K.E., Hurford, A., and Moise, E.R.D. 2023. Species distribution model identifies influence of climatic constraints on severe defoliation at the leading edge of a native insect outbreak. For. Ecol. Manage. **544**: 121166. doi:10.1016/j.foreco.2023.121166.

Zhang, B., MacLean, D.A., Johns, R.C., and Eveleigh, E.S. 2018. Effects of hardwood content on balsam fir defoliation during the building phase of a spruce budworm outbreak. Forests **9**: 530. doi:10.3390/f9090530.

Zhang, B., MacLean, D.A., Johns, R.C., Eveleigh, E.S., and Edwards, S. 2020. Hardwood-softwood composition influences early-instar larval dispersal mortality during a spruce budworm outbreak. For. Ecol. Manage. **463**: 118035. doi:10.1016/j.foreco.2020.118035.

Zhao, K., MacLean, D.A., and Hennigar, C.R. 2014. Spatial variability of spruce budworm defoliation at different scales. For. Ecol. Manage. **328**: 10–19. doi:10.1016/j.foreco.2014.05.020.

Zuur, A.F., Ieno, E.N., Walker, N.J., Saveliev, A.A., and Smith, G.M. 2009. Mixed Effects Models and Extensions in Ecology with R. New York, NY: Springer.

849 **Table 1.** Description of 23 plot-level explanatory variables (fixed effects) grouped by stand, site
850 and climate categories examined for their influence on balsam fir current and cumulative
851 defoliation patterns using mixed effects models. Model random effect structure included sample
852 plots nested with stands and year as a crossed random effect.

	Explanatory Variables	Description	$\bar{\chi}$	σ
Stand	Sprayed	Annual aerial spraying of insecticides		
	L2branch	Spatially interpolated estimates of SBW L2 populations per branch	19.5	13.9
	BFba	Balsam fir basal area (m^2/ha)	26.9	12.2
	WSba	White spruce basal area (m^2/ha)	2.8	4.8
	BSba	Black spruce basal area (m^2/ha)	5.6	9.7
	HWba	Hardwood basal area (m^2/ha)	7.1	8.9
	Totalba	Total basal area (m^2/ha)	43.2	6.8
Site	Elevation	Ground elevation above sea-level (m)	284	65
	Aspect	Compass direction of downward slope (0–360 degrees)	239	90
	Slope	Inclination of downward slope (0–90 degrees)	5.2	3.8
	RootDep	Rooting depth (3 classes <20cm, 20–40cm, >40cm)		
	SoilQual	Soil nutrient/moisture quality (6 classes used out of 9 possible classes)		
	DTW	Depth-to-water index (0–55, lower values equate to water near surface)	11.9	11.7
Climate	SpCDD	Spring cumulative degree days >5°C from Apr.–May	133.7	32.5
	SuCDD	Summer cumulative degree days >5°C from Jun.–Jul.	663.0	41.5
	SpMinTp	Summed spring monthly minimum temperature from Apr.–May	-19.2	3.4
	SuMinTp	Summed summer monthly minimum temperature from Jun.–Jul.	6.4	2.8
	WiMinTp	Summed winter monthly minimum temperature from Nov.–Mar.	-124.9	10.0
	SpMaxTp[a]	Summed spring monthly maximum temperature from Apr.–May	44.2	4.8
	SuMaxTp[b]	Summed summer monthly maximum temperature from Jun.–Jul.	59.4	3.2
	WiMaxTp[a]	Summed winter monthly maximum temperature from Nov.–Mar.	34.1	9.3
	SpPrcp	Summed spring monthly precipitation (mm) from Apr.–May	182.1	43.7
	SuPrcp[b]	Summed summer monthly precipitation (mm) from Jun.–Jul.	188.3	52.1

853 * Sprayed, L2branch and all climate variables include annual plot-level observations.
854 [a,b] The same superscripts indicate pair-wise collinearity (r >0.70) between explanatory variables.

855 **Table 2.** Overall spatial autocorrelation trends at varying distances for balsam fir current
856 defoliation per plot within stands (100–600m) and between stands (1000–20,000m) based on
857 global Moran's *I*. Bolded values indicate highest results per year and asterisks signify not
858 rejecting null hypothesis due to randomness of defoliation patterns.

	Balsam fir current defoliation global Moran's *I* by distance (m)										
	Plots within stands						Plots between stands				
Year	100	200	300	400	500	600	1000	2500	5000	10000	20000
2011	**0.48**	0.46	0.44	0.43	0.44	0.46	0.43	0.37	0.23	0.22	0.22
2012	0.41	0.57	**0.58**	0.55	0.54	0.52	0.45	0.45	0.30	0.25	0.25
2013	0.69	**0.77**	0.75	0.74	0.70	0.66	0.53	0.29	0.05	0.04	0.03
2014	**0.82**	0.81	0.80	0.80	0.76	0.72	0.63	0.21	0.01*	-0.02*	-0.02*
2015	0.83	**0.85**	**0.85**	**0.85**	0.84	**0.85**	0.84	0.51	0.08	-0.02*	-0.02*
2016	0.93	**0.94**	**0.94**	0.93	0.93	0.91	0.87	0.63	0.33	0.17	0.17
2017	**0.83**	0.74	0.71	0.69	0.64	0.58	0.50	0.42	0.30	0.20	0.20
2018	**0.86**	0.85	0.82	0.81	0.75	0.65	0.45	0.22	0.03*	0.01*	0.02*
2019	0.83	**0.84**	0.83	**0.84**	**0.84**	**0.84**	0.81	0.72	0.25	0.05	0.05
2020	0.70	0.84	**0.85**	0.82	0.81	0.80	0.78	0.63	0.20	-0.01*	-0.02*
2021	0.85	**0.88**	0.87	0.86	0.85	0.85	0.81	0.72	0.51	0.01*	-0.02*

859

Table 3. Spatial autocorrelation Getis-Ord *Gi** analysis of balsam fir current defoliation per year: proportion of plots labelled as 'hot spots' (highly defoliated plots surrounded by other highly defoliated plots) and 'cold spots' (lightly defoliated plots surrounded by other lightly defoliated plots), or not significantly clustered ($\alpha = 0.05$) using a maximum within stand plot distance of 600m. Number of plots (n) per year declined over time due to timber harvesting.

Balsam fir current defoliation hot/cold spot analysis of sample plots (%)				
Year	n	Hot spots	Cold spots	Not clustered
2011	84	14	6	80
2012	84	20	10	70
2013	84	19	13	68
2014	84	25	21	54
2015	84	13	23	64
2016	84	14	25	61
2017	75	7	21	72
2018	75	17	12	71
2019	57	18	23	59
2020	54	6	17	77
2021	54	19	19	62

Table 4. Generalized and linear mixed models (GLMM, LMM) examining relationships between balsam fir current and cumulative defoliation (response variables) and site, stand, and climate explanatory variables. Model analyses using maximum likelihood estimation applied stepwise forward explanatory variable selection considering model goodness-of-fit Akaike and Bayesian Information Criterion (AIC, BIC), and analysis of variance likelihood ratio tests. Marginal and conditional R^2 and root mean squared error are based on restricted maximum likelihood estimation. ***Bolded*** and ***italicized*** text identifies the final models selected based on lowest BIC.

Model ~ Explanatory variables	AIC	BIC	Likelihood ratio test p-value	Marg. R^2	Cond. R^2	RMSE
LMM: Balsam fir cumulative defoliation						
M1 ~ Sprayed	8810	8838		0.014	0.938	43.066
M2 ~ Sprayed + SuMinTp	8807	8840	0.021	0.020	0.933	42.945
M3 ~ Sprayed + SuMinTp + WiMaxTp	8802	8840	0.008	0.054	0.933	42.765
M4 ~ Sprayed + SuMinTp + WiMaxTp + SuMaxTp	8799	8841	0.024	0.110	0.928	42.667
M4a ~ Sprayed + SuMinTp + SuMaxTp + L2branch*HWba	8754	8806	<0.0001	0.066	0.929	41.306
M4b ~ Sprayed + SuMinTp + SuMaxTp + HWba + WSba + L2branch*HWba + L2branch*WSba	***8712***	***8773***	***<0.0001***	***0.085***	***0.931***	***40.186***
M5 ~ Sprayed + SuMinTp + WiMaxTp + SuMaxTp + Totalba	8797	8844	0.051	0.111	0.928	42.691
M6 ~ Sprayed + SuMinTp + WiMaxTp + SuMaxTp + Totalba + BFba	8795	8847	0.045	0.111	0.928	42.692
GLMM: Balsam fir current defoliation						
M1 ~ Sprayed	4430	4454		0.031	0.340	0.176
M2 ~ Sprayed + L2branch	4340	4368	<0.0001	0.053	0.281	0.173
M3 ~ Sprayed + L2branch + WiMaxTp	4242	4274	<0.0001	0.205	0.557	0.167
M4 ~ Sprayed + L2branch + WiMaxTp + SuMinTp	4223	4260	<0.0001	0.268	0.629	0.166
M5 ~ Sprayed + L2branch + WiMaxTp + SuMinTp + SuMaxTp	4214	4257	0.0012	0.227	0.604	0.165
M5a ~ Sprayed + L2branch + WiMaxTp + SuMinTp + SuMaxTp + Sprayed*SuMinTp	4141	4188	<0.0001	0.209	0.582	0.161
M5b ~ Sprayed + L2branch + WiMaxTp + SuMinTp + SuMaxTp + HWba + Sprayed*SuMinTp + L2branch*HWba	***4100***	***4156***	***<0.0001***	***0.193***	***0.542***	***0.160***
M6 ~ Sprayed + L2branch + WiMaxTp + SuMinTp + SuMaxTp + SpPrcp	4210	4257	0.014	0.230	0.575	0.165
M7 ~ Sprayed + L2branch + WiMaxTp + SuMinTp + SuMaxTp + SpPrcp + SpMaxTp	4207	4259	0.028	0.191	0.507	0.165

Note: See Table 1 for description of model explanatory variables. Models M4a and M4b (cumulative defoliation) and M5a and M5b (current defoliation) evaluated adding interactions among explanatory variables.

873 **Table 5**. Summaries for final generalized and linear mixed-effects models (GLMM, LMM)
874 examining the effects of site, stand, and climate explanatory variables on balsam fir current and
875 cumulative defoliation response variables. Coefficient mean estimates and log-odds (converted
876 probabilities) are based on standardized z-scores along with standard errors and significance.

LMM: Balsam fir cumulative defoliation

Fixed effect variables	Mean estimate	Std. error	t-value	p-value
Intercept	225.30	43.33	5.20	0.0003
Sprayed	-84.08	6.78	-12.40	<0.0001
SuMinTp	-19.33	5.81	-3.33	0.0009
SuMaxTp	29.83	11.34	2.63	0.0087
HWba	-17.09	7.55	-2.26	0.0282
WSba	-10.37	4.09	-2.54	0.0133
L2branch*HWba	-15.22	1.65	-9.25	<0.0001
L2branch*WSba	-8.53	1.32	-6.47	<0.0001

GLMM: Balsam fir current defoliation

Fixed effect variables	Log-odds (probability)	Std. error	z-value	p-value
Intercept	-0.26 (0.43)	0.46	-0.57	0.57
Sprayed	-1.53 (-0.18)	0.11	-13.39	<0.0001
L2branch	0.48 (0.62)	0.04	11.41	<0.0001
SuMinTp	-0.17 (-0.46)	0.09	-1.99	0.0002
SuMaxTp	-0.61 (-0.35)	0.16	-3.92	<0.0001
WiMaxTp	1.02 (0.73)	0.13	7.62	<0.0001
HWba	-0.17 (0.46)	0.09	-1.96	0.05
Sprayed*SuMinTp	-0.94 (-0.28)	0.12	-8.05	<0.0001
L2branch*HWba	-0.16 (-0.46)	0.03	-6.28	<0.0001

877 **Note:** Abbreviations for fixed effect explanatory variables are listed in Table 1. Alternative
878 model formulations used to select the final model based on lowest Bayesian Information
879 Criterion (BIC) are presented in (Table 4). To convert the standardized model coefficients back
880 to their original values/units, the formula is: $X = Z * (\sigma_x + \mu_x)$ where Z is the standardized value.

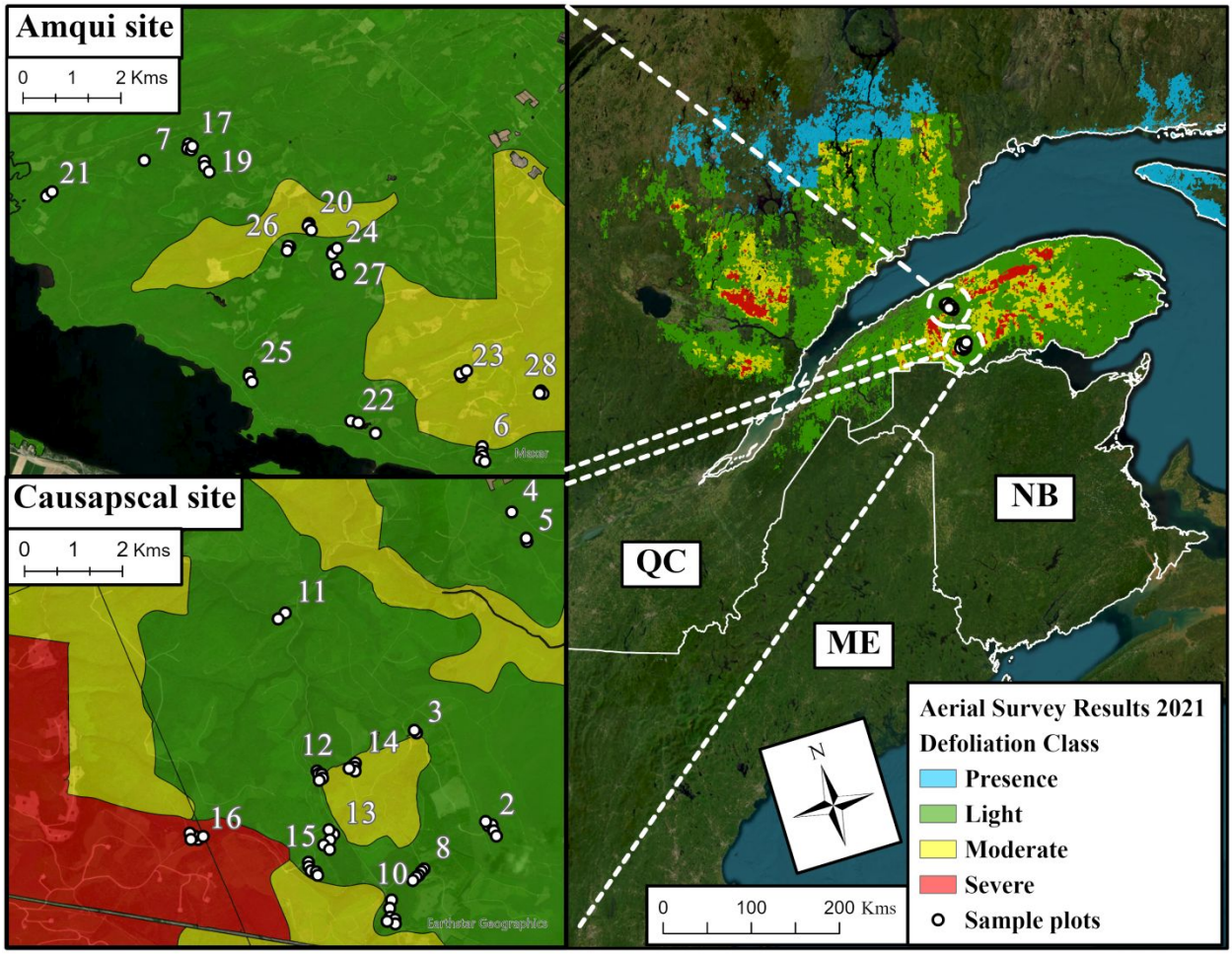

881

882 **Fig. 1.** Study area for two sites containing the 87 sample plot locations (Amqui n = 40 and
883 Causapscal n = 47) overlaid on Québec government aerial surveys of spruce budworm
884 defoliation classes from 2021 (MRNF, 2021). Groups of sample plots are labelled by their
885 corresponding stand number; data on characteristics of each stand are included in Supplementary
886 Table S1. Figure created using ArcGIS Pro 3.3.2. (ESRI, 2023) with base map satellite imagery
887 (ESRI), aerial survey defoliation layer (MRNF, 2021), and overlaid points for plot locations in
888 the WGS 1984 UTM 19N projection.

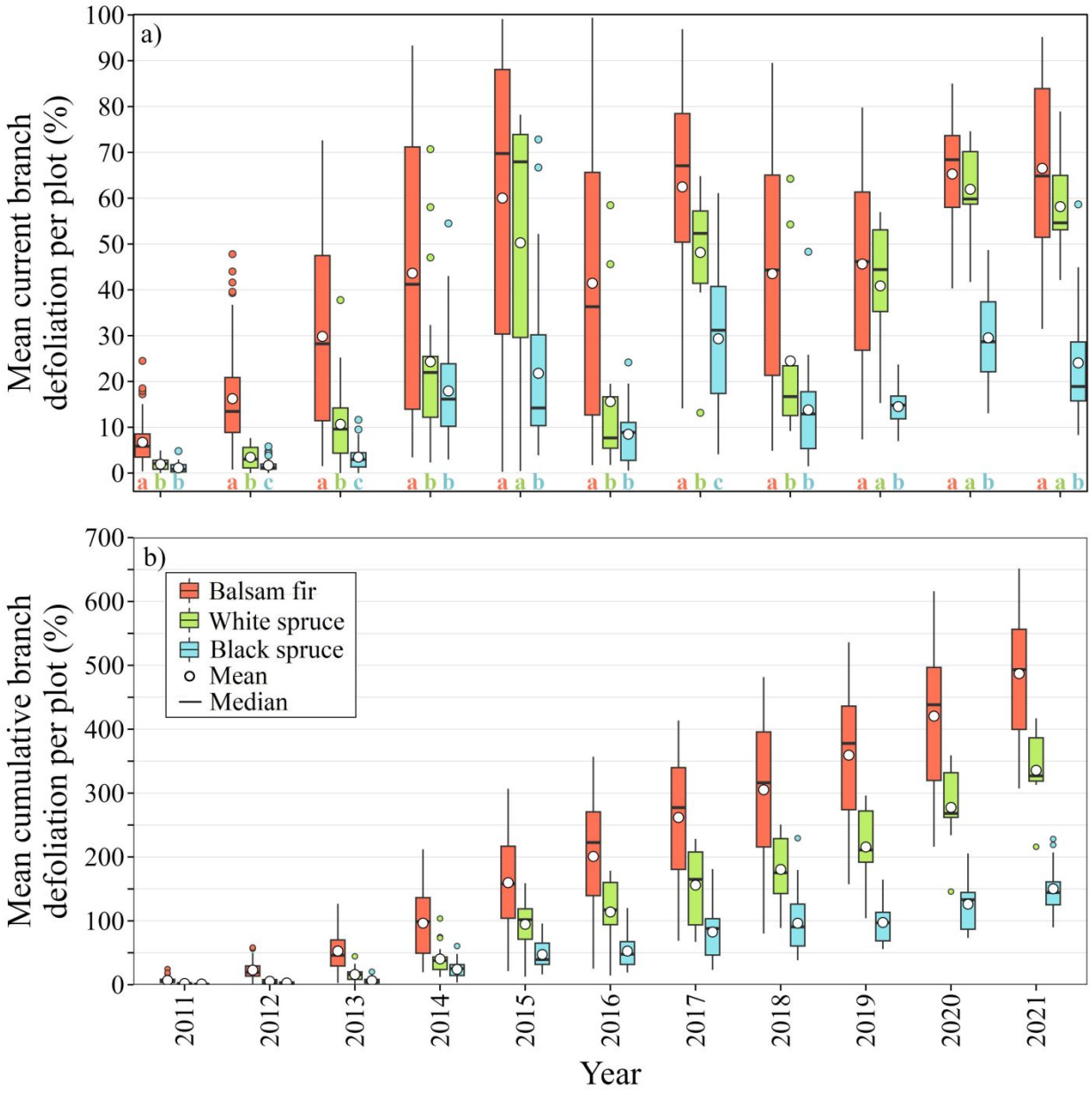

Fig. 2. Box plots showing (a) mean current defoliation and (b) mean cumulative defoliation by spruce budworm host tree species (balsam fir, white spruce, and black spruce) for 87 sample plots from 2011–2021. Colored letters at bottom of panel a) indicate significant differences of means among species per year using Games-Howell pairwise comparison test. Cumulative defoliation was calculated by summing mean current annual defoliation.

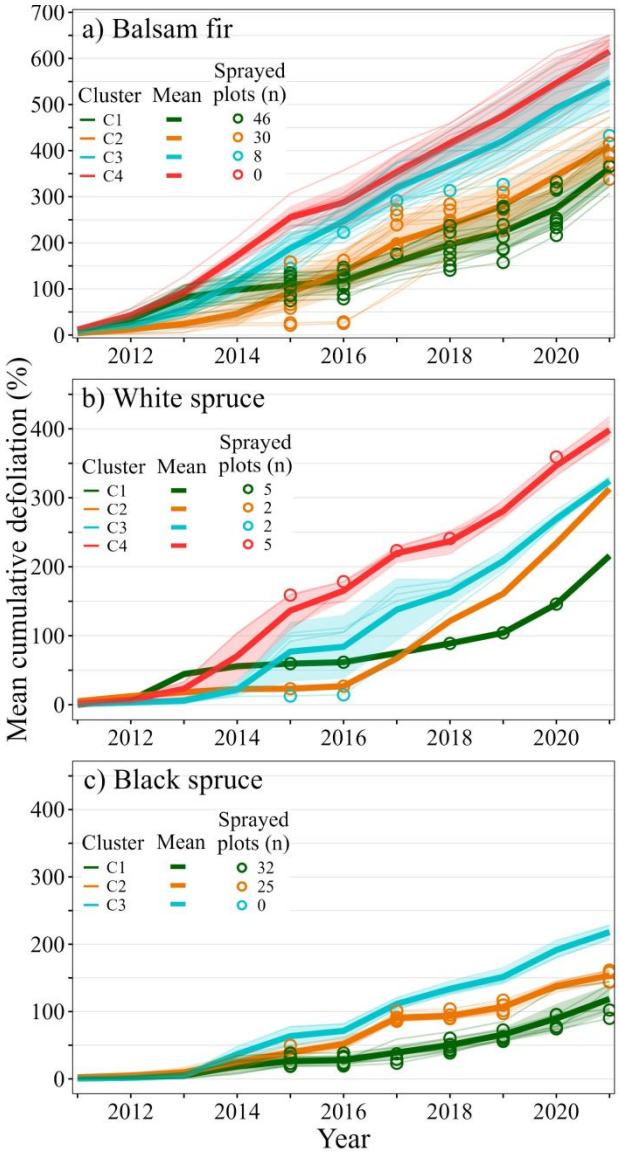

Fig. 3. Hierarchical cluster analysis results for cumulative defoliation patterns of plots from 2011–2021 of (a) balsam fir, (b) white spruce, and (c) black spruce. Shaded bands represent ± 1 standard deviation of the mean per cluster, fine lines show individual plots, and circles indicate years of annual aerial spraying of insecticide per plot.

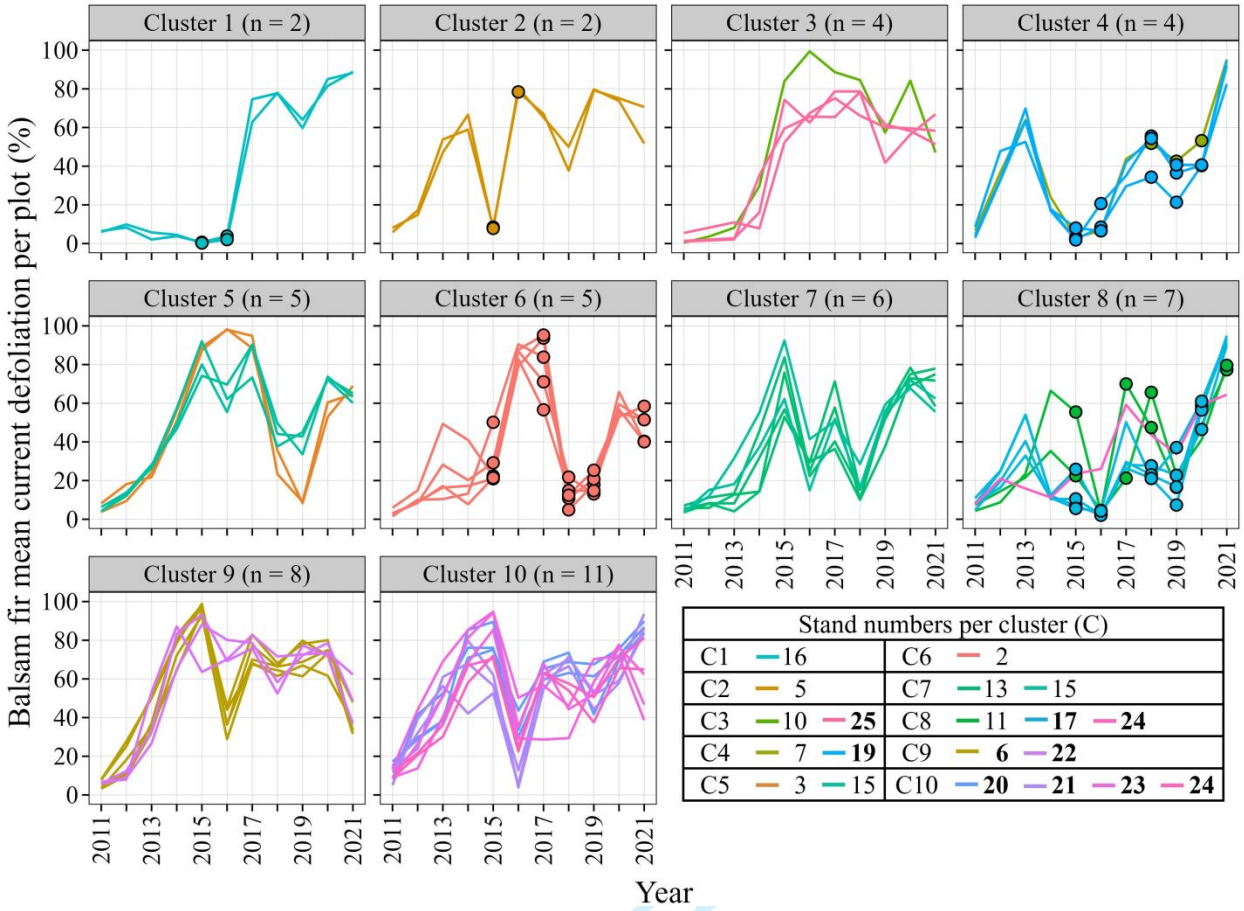

Fig. 4. Hierarchical cluster analysis results for current defoliation patterns from 2011–2021 of balsam fir. Each panel represents a cluster of plot defoliation patterns that are colored by stand number. Circles indicate years of annual aerial spraying of insecticide per plot and bold numbers in the legend indicate stands located in the Amqui site.

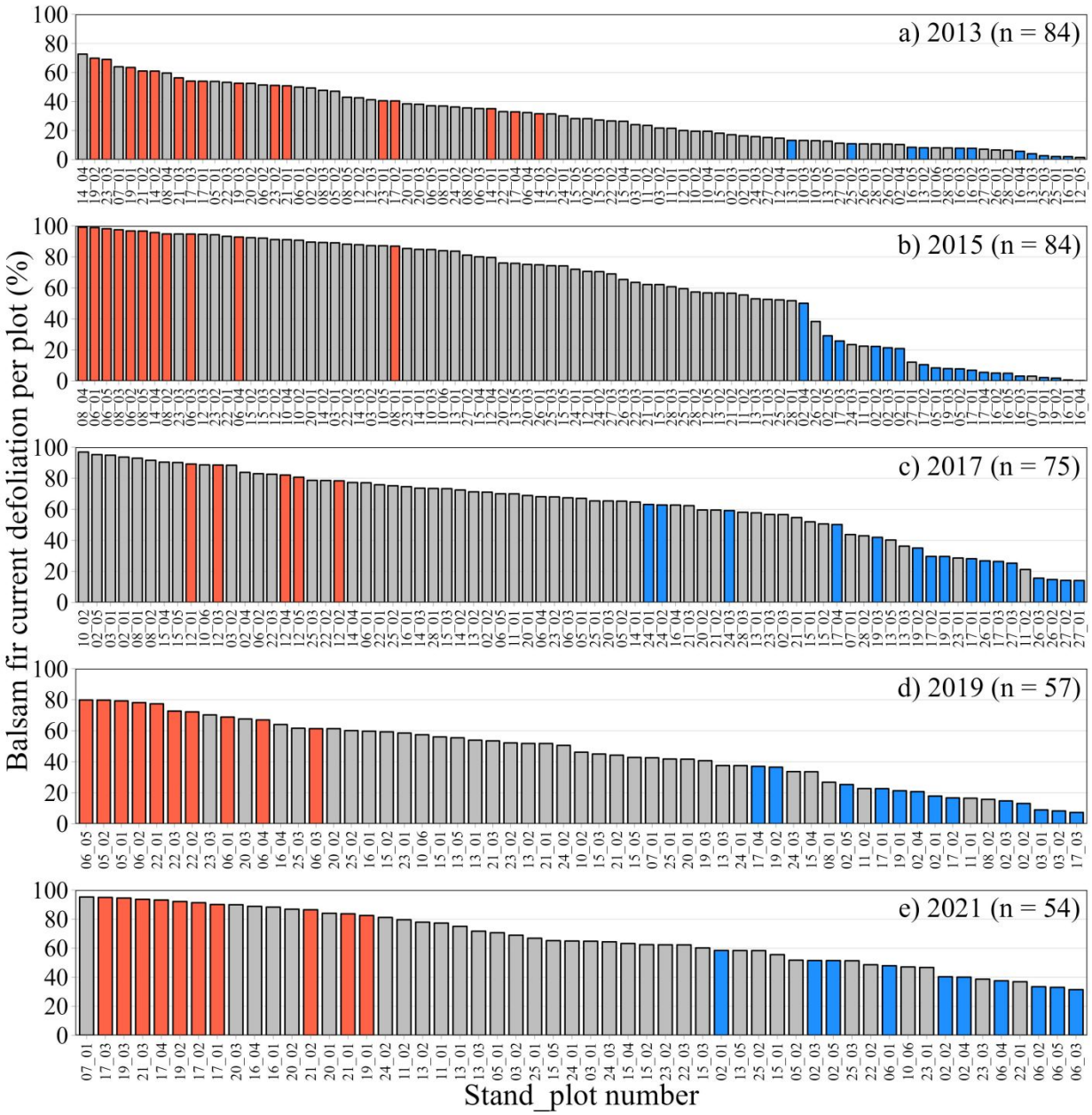

907

908 **Fig. 5.** Mean balsam fir current defoliation for plots, ordered from highest to lowest defoliation
909 for every second year from 2013 to 2021. Plots showing significantly clustered within stand
910 defoliation ($\alpha = 0.05$) are colored red ('hot spots' - highly defoliated plots surrounded by other
911 highly defoliated plots) and blue ('cold spots' - lightly defoliated plots surrounded by other
912 lightly defoliated plots), or grey (not significantly clustered)), based on Getis-Ord *Gi** analysis.
913 Number of plots per year declined due to timber harvesting.

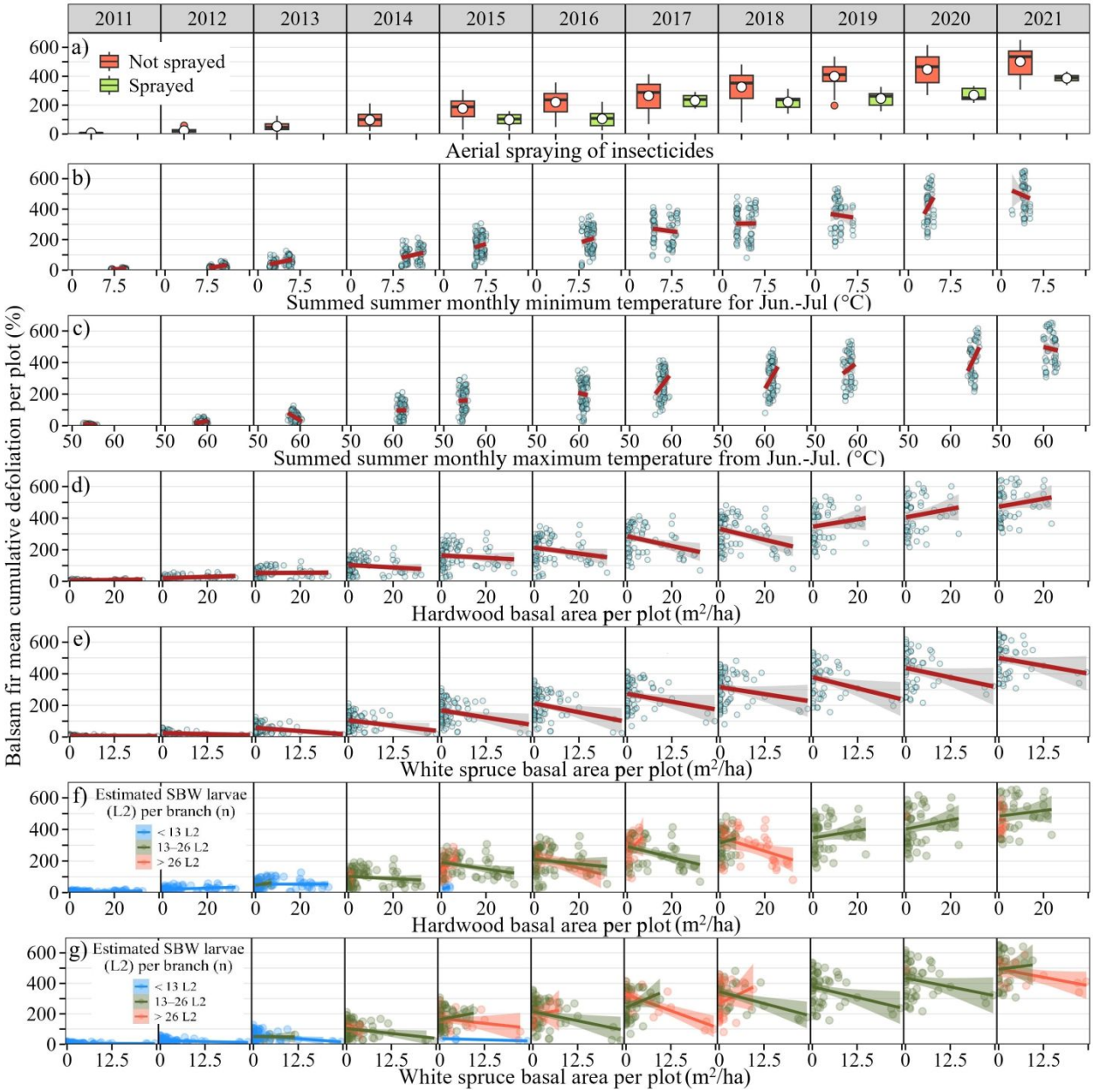

914

915 **Fig. 6.** Fitted linear relationships between annual balsam fir mean cumulative defoliation per plot
916 and significant explanatory variables: a) annual spraying of insecticides; b) summer monthly
917 minimum temperature; c) summer monthly maximum temperature; d) hardwood basal area per
918 plot; e) white spruce basal area per plot; f) interaction between hardwood basal area and SBW L2
919 per branch; and g) interaction between white spruce basal area and SBW L2 per branch.

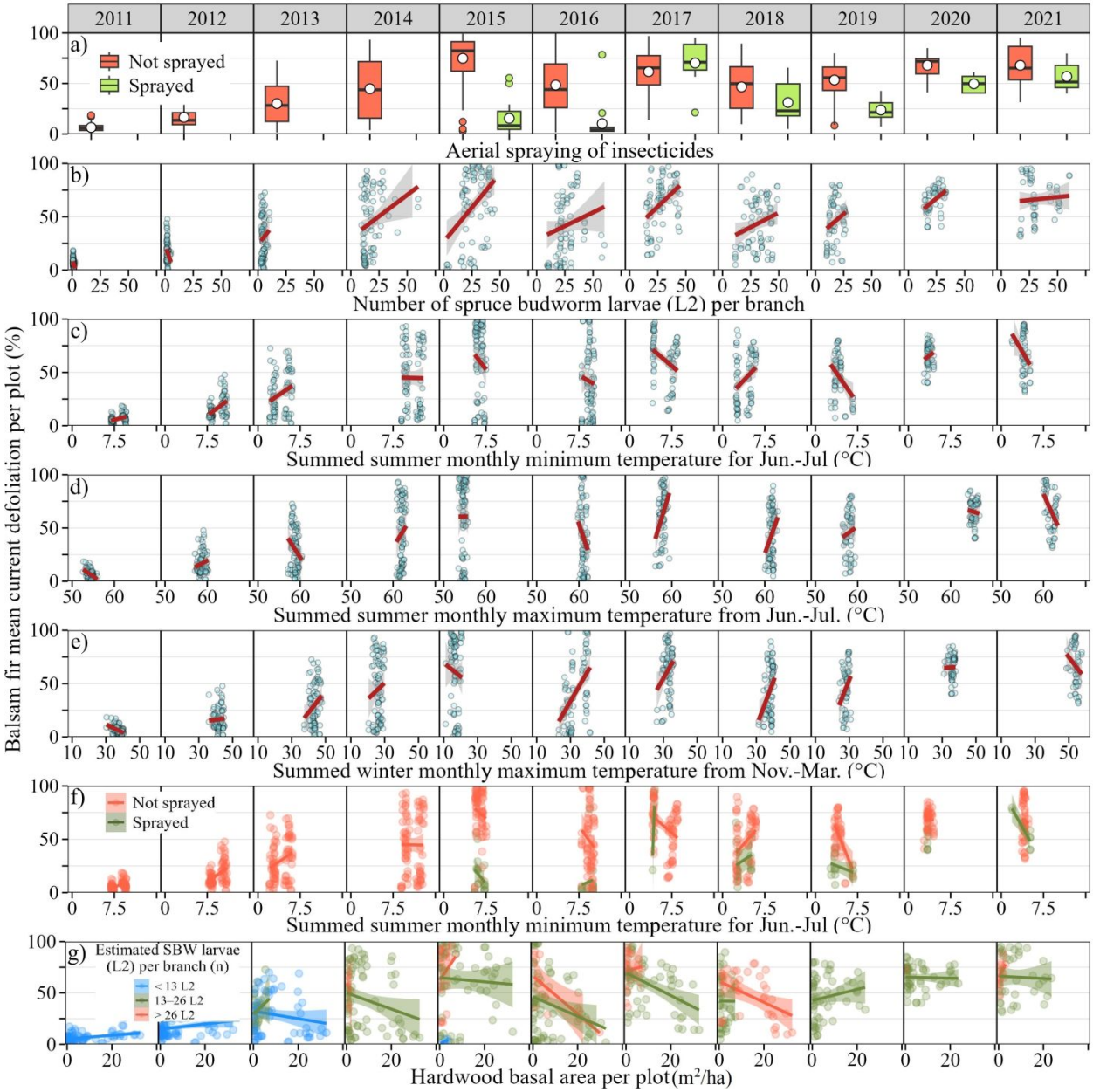

Fig. 7. Fitted linear relationships between annual balsam fir mean current defoliation per plot and significant explanatory variables: a) spraying of insecticides; b) SBW L2 populations per branch; c) summer monthly minimum temperature; d) summer monthly maximum temperature; e) winter monthly maximum temperature; f) interaction between spraying insecticides and summer cumulative degree days; and g) interaction between hardwood basal area and SBW L2.